

Real-time measurement in slow displacement of the tunnel floor due to dynamic ground motion at the KEKB injector linac

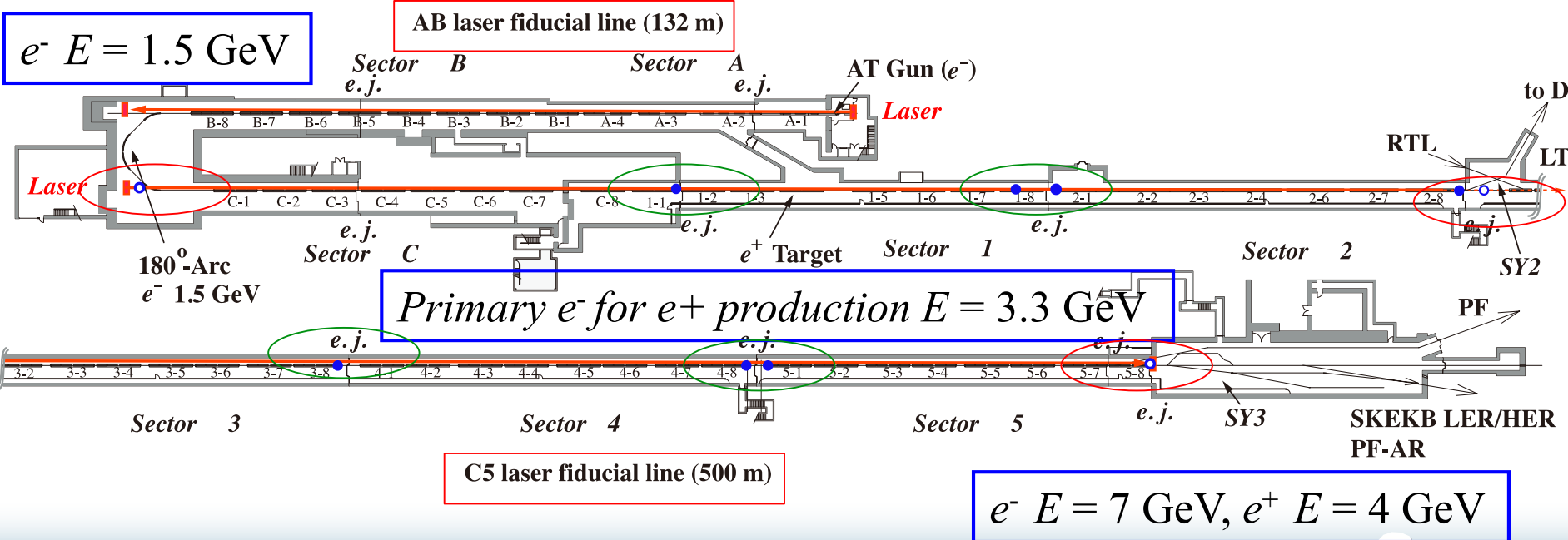
T. Suwada, Y. Enomoto, K. Kakihara, K. Mikawa, T. Higo,
Accelerator Laboratory, KEK, Tsukuba, Japan

Introduction

- High-precision laser-based alignment is one of the important issues in the KEKB linac upgrade towards the Super KEK B-factory.
- The implementation of the laser-based alignment started in the summer of 2013, and the initial alignment finished in Jan. 2015.
- A new remote sensing system is in progress to measure slow displacement of the tunnel floor due to dynamic ground motion in real time.
- Based on the recent measurements, we have found that the transverse displacements of the floor level with respect to the laser axis are not negligibly small.
- In this report, the measurement and analysis results are described in detail in slow displacement of the tunnel floor at the KEKB injector linac.

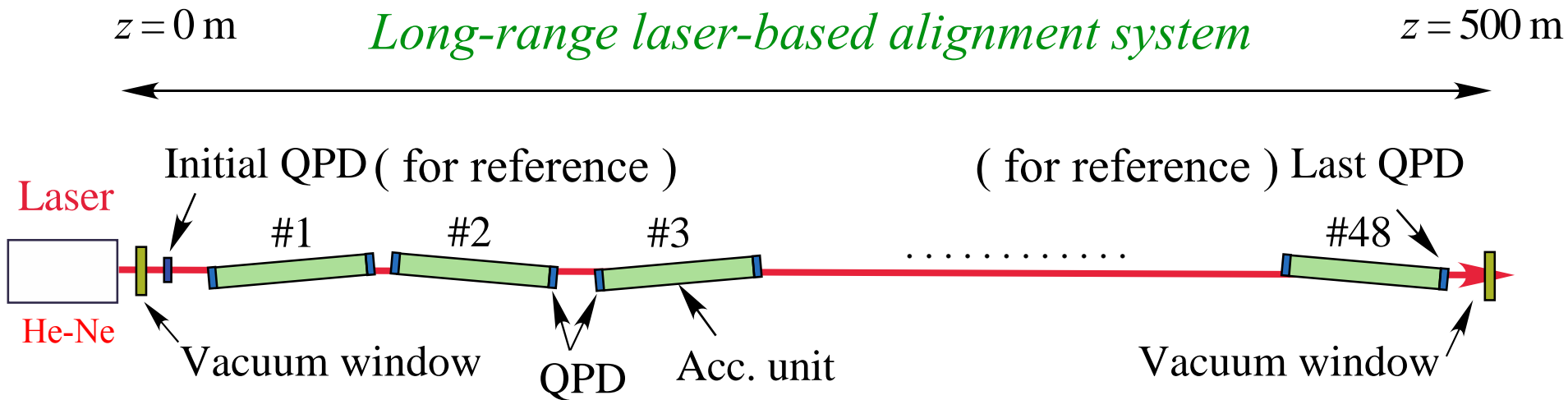
KEKB linac layout and the laser-based alignment system

- Two long straight sections, AB (125m) and C5 (475m) sections with independent laser sources (He-Ne) and quadrant silicon photodiodes (QPDs).
- Two (seven) remote-controllable QPDs were installed in the summer shutdown of 2014 (2015) at multiple locations just near expansion joints (*e.j.*) of the linac building (see Table 1).



M. Akemoto, et al., Prog. Theor. Exp. Phys. 2013 , 03A002.

Alignment measurement scheme for girders and components



- *Long-range alignment system for girders* (accuracy $\sigma \sim 100\mu\text{m}$)
The girder units can be aligned with a laser-based alignment system.
- *Short-range alignment system for components* (accuracy $\sigma \sim 50\mu\text{m}$)
The accelerator components on a girder unit are aligned with a standard laser-tracker technique.

Table of new remote-controllable QPDs

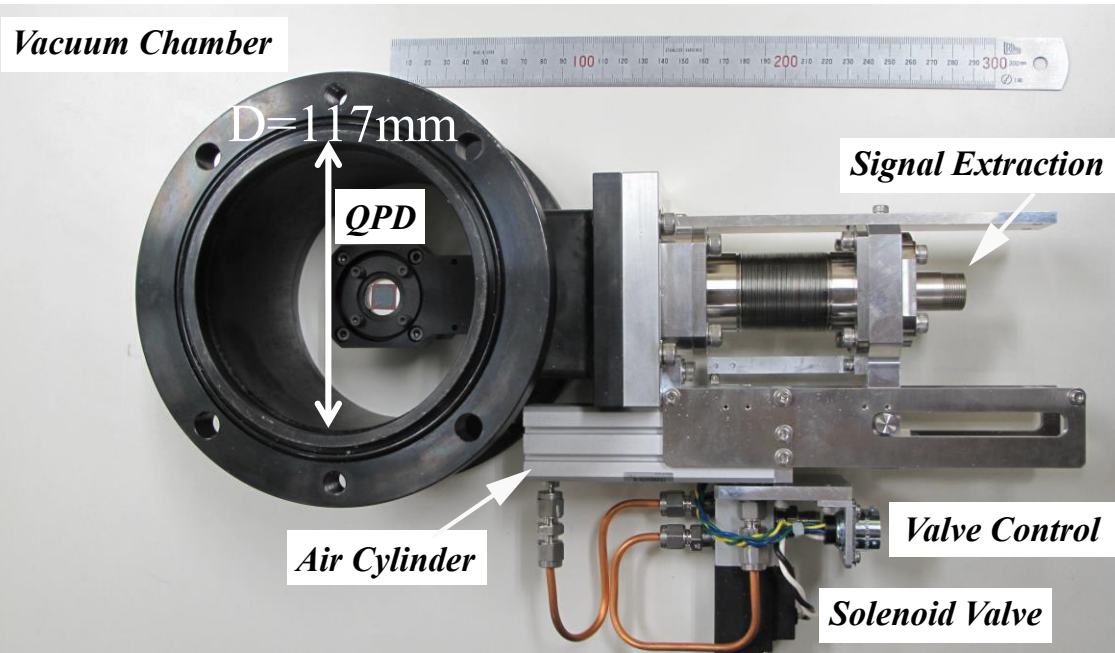
QPD	<i>e.j.</i>	<i>L</i> [m]	<i>r_m</i> [mm]	<i>s_r</i> [μm/day]
REF1UA		1.74	0.19	3.3
	C3D	44.31	—	—
11DA		106.11	0.55	5.5
	11D	106.72	—	—
1814DA		177.04	0.65	5.1
	1814D	178.39	—	—
21UA		180.17	0.47	4.2
28G6DA		259.07	0.65	6.6
	28G6D	259.64	—	—
28REFUA		263.32	0.44	4.1
38DA		339.58	0.68	4.1
	38G5U	341.60	—	—
48DA		419.08	0.88	4.6
	48G5U	421.11	—	—
51UA		423.65	0.84	5.1
	57G7U	498.01	—	—
584D		499.94	—	—

(fixed reference QPD)

1. Summary table in the locations of the remote controllable QPDs, and expansion joints (*e.j.*) along the injector linac from the laser source.
1. Some measurement results, the maximum norm (*r_m*) of the displacement vector and the maximum slope (*s_r*) in the variations in the time traces of the norm, are also summarized depending on the QPD locations.

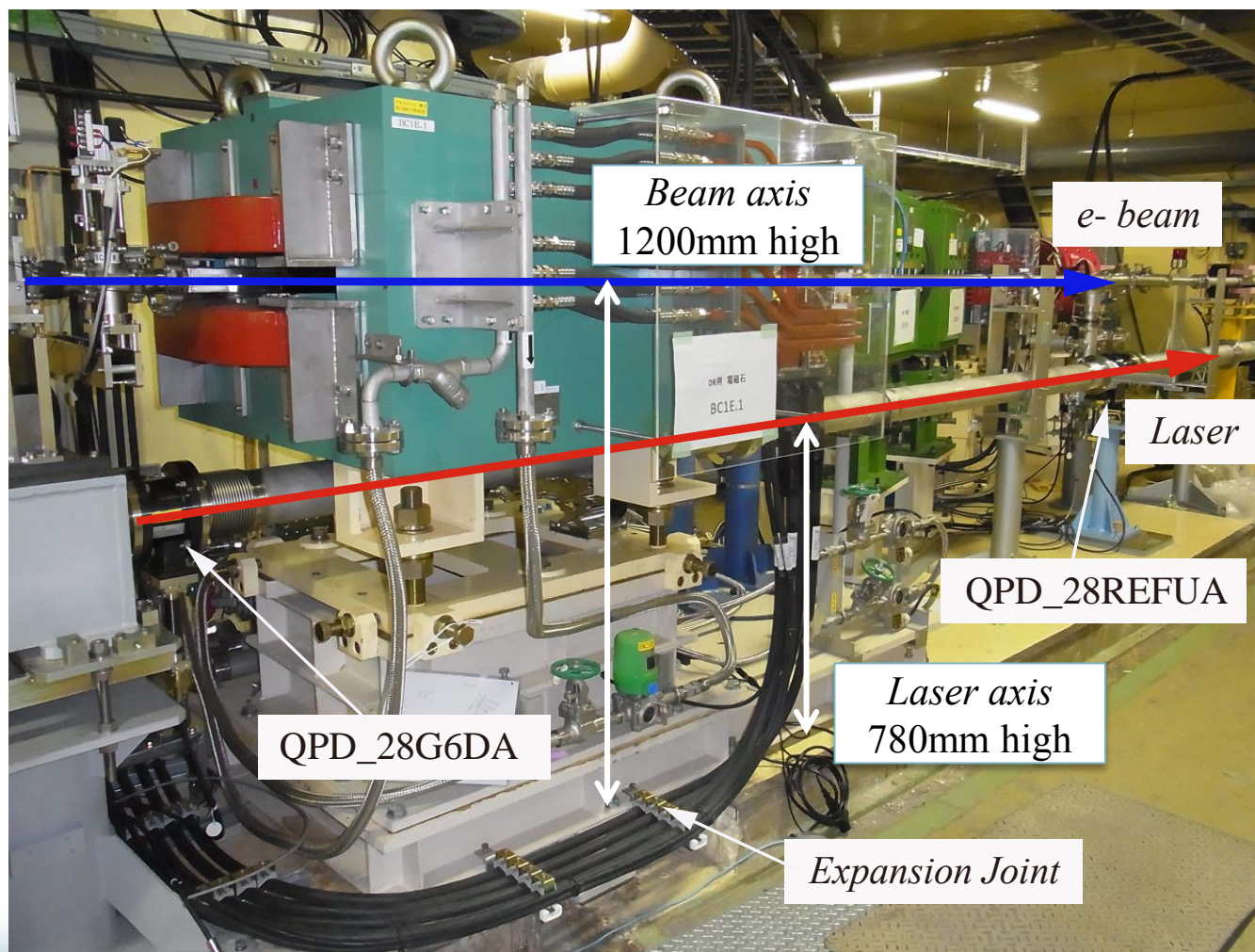
○ reference QPDs

Developed Remote-Controllable Quadrant Silicon Photodiode (QPD)

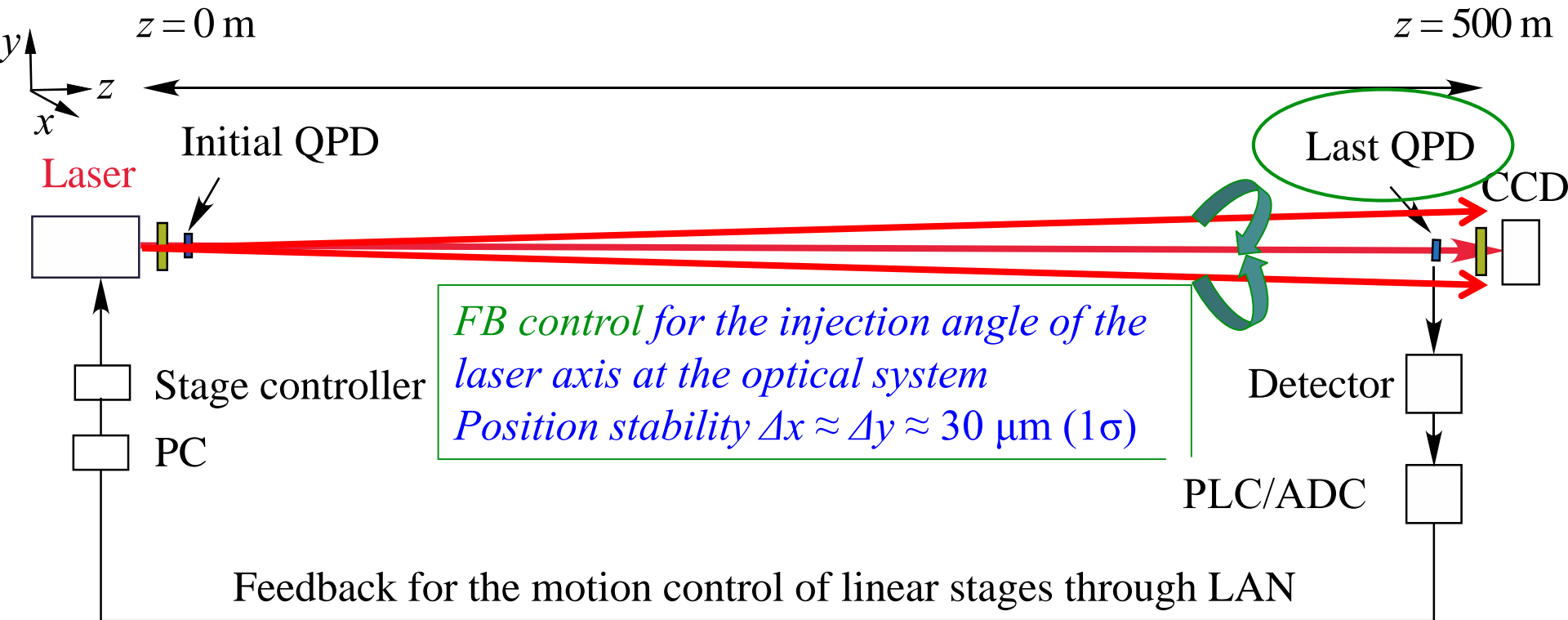


- A remote-controllable QPD sensor, QPD: OSI Optoelectronics, SPOT-9D (D = 10mm ϕ)
- Aperture D = 117 mm (effect. aperture D = 92 mm)
- Actuator-based QPD driving system with a compact air cylinder and a micro-solenoid valve driven by a compressed air

Remote-controllable QPDs installed at SY2



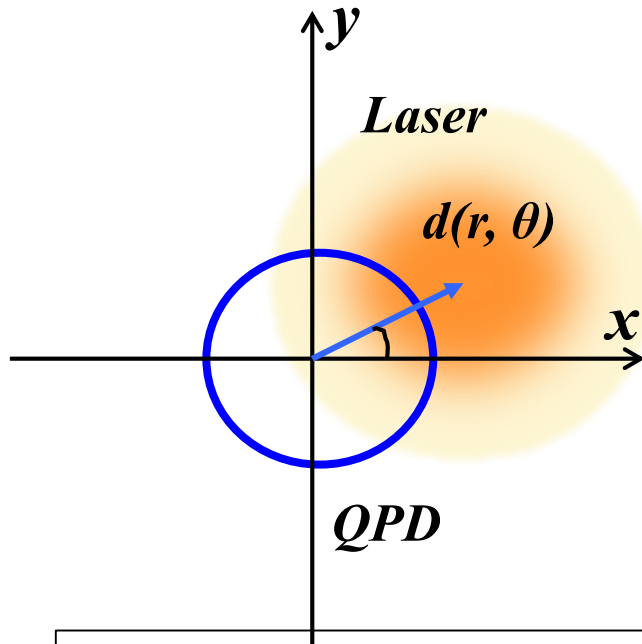
Feedback control for stabilizing an injection laser axis



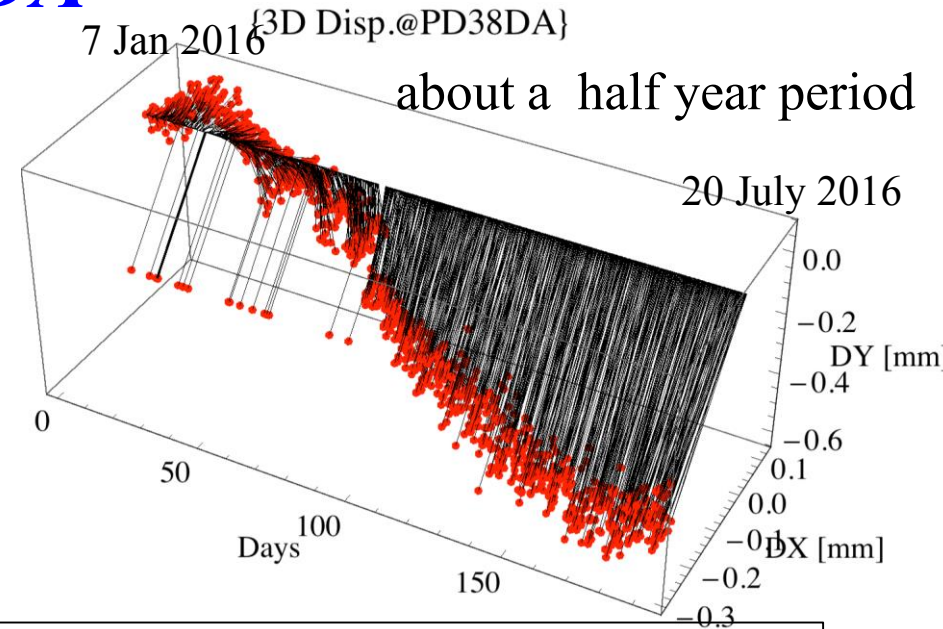
Stage with pico-motors for $f5000$ lens (Crucial for stable laser axis)

- M-562-XYZ/Newport, translational resolution 30nm/step $\rightarrow \sim 1\text{rad}/\text{step}$
- The drive shaft is rotated by frictional force of piezoelectric element and the stage translates in the transverse plane.

Time trace of a typical displacement vector @ QPD-38DA



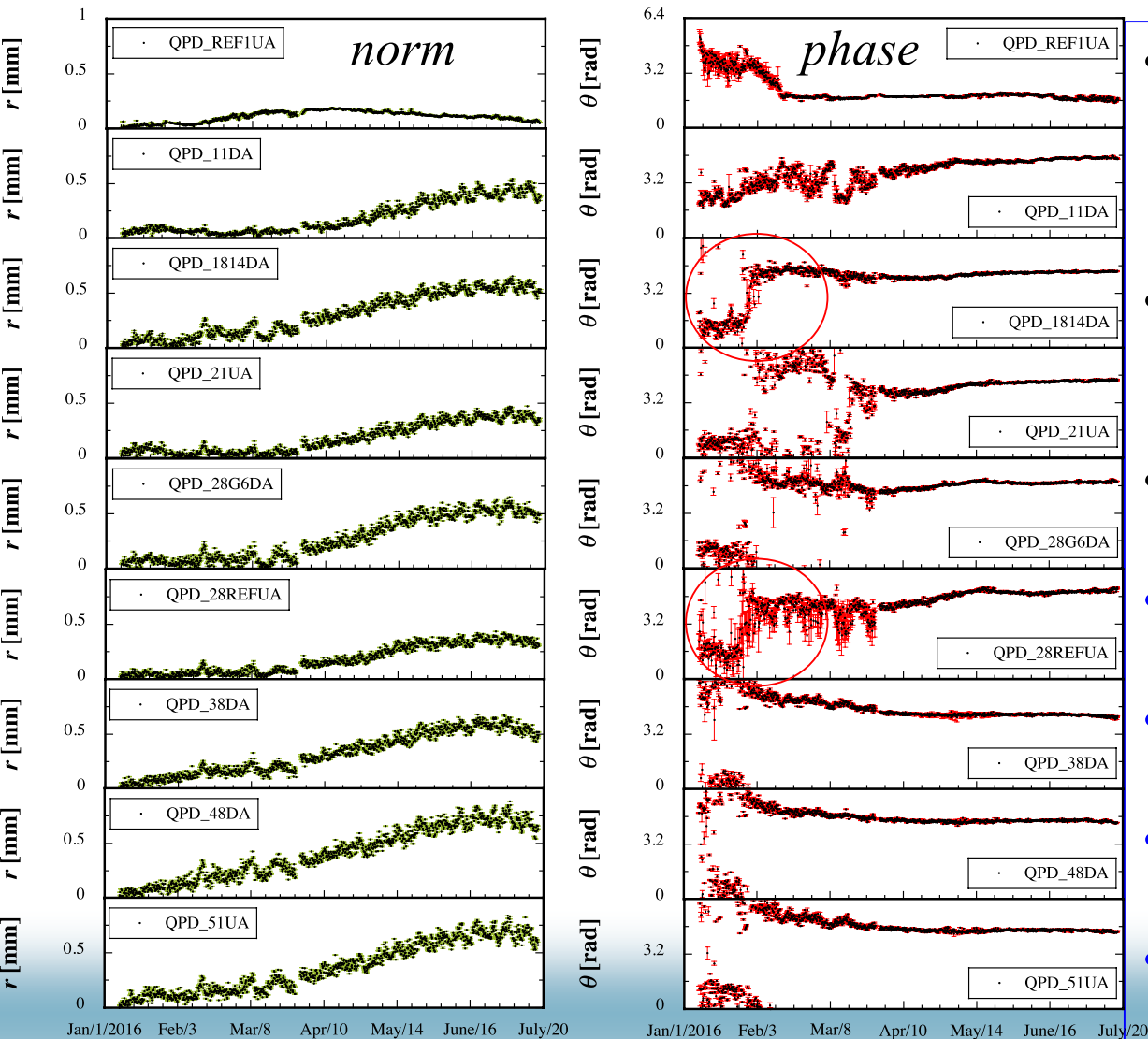
displacement vector d



differential displacement vector

- Every four hours on the hour, the basic functions provided by the server start to work in order to take a series of the displacement data for all the remote QPDs.
- The results show typical variations in a time trace of the displacement vector with a feedback control on.
- It can be seen that the displacement vector has complicatedly rotated around the laser axis along with the growth of the vector norm in the time direction.

Time traces of all the displacement vectors



- Norm and phase of the displacement vectors for all the accelerator units with feedback control on.
- The phase is defined by an angular range of $0-2\pi$.
- Data taking period: 7 Jan – 20 July 2016.
- *Max. norm:*
 $r_{max} = 0.19 - 0.88$ mm
- *Average max. norm:*
 $\langle r_{max} \rangle = 0.65$ mm
- *Max. growth rate:*
 $sr = 3.3 - 6.6$ $\mu\text{m}/\text{day}$
- *Average max. growth rate:*
 $\langle sr \rangle = 4.9$ $\mu\text{m}/\text{day}$

Cross-correlation analysis between the displacement vectors

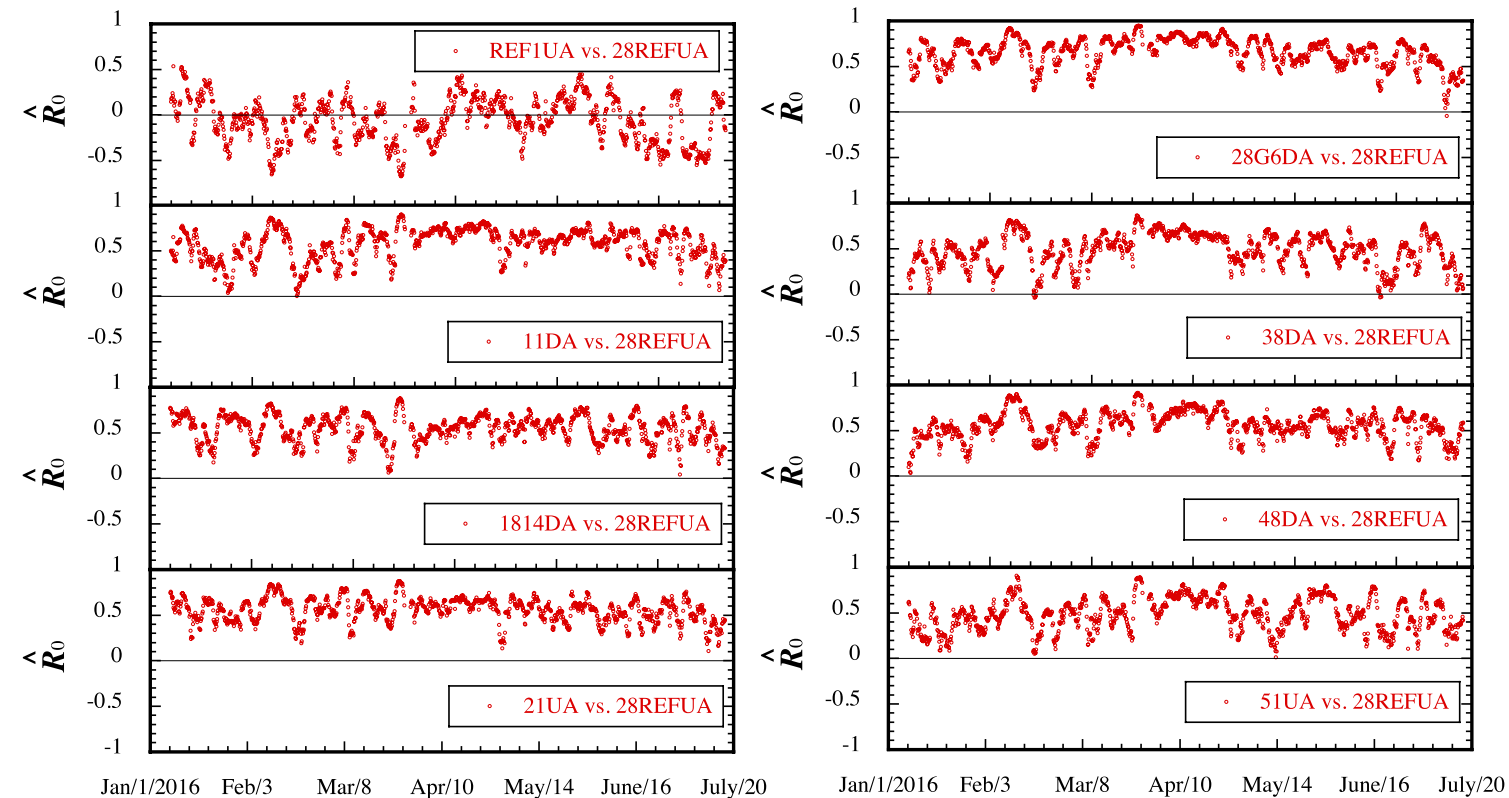
$$\langle \vec{\mu}(i) \rangle = \frac{1}{N} \sum_{n=1}^N \vec{d}_n(i), \quad (1)$$

$$\hat{C}_k(i, j) = \frac{1}{N} \sum_{n=1}^N (\vec{d}_n(i) - \langle \vec{\mu}(i) \rangle) \cdot (\vec{d}_{n-k}(j) - \langle \vec{\mu}(j) \rangle), \quad (2)$$

$$\hat{R}_k(i, j) = \frac{\hat{C}_k(i, j)}{\sqrt{\hat{C}_0(i, i) \hat{C}_0(j, j)}}. \quad (3)$$

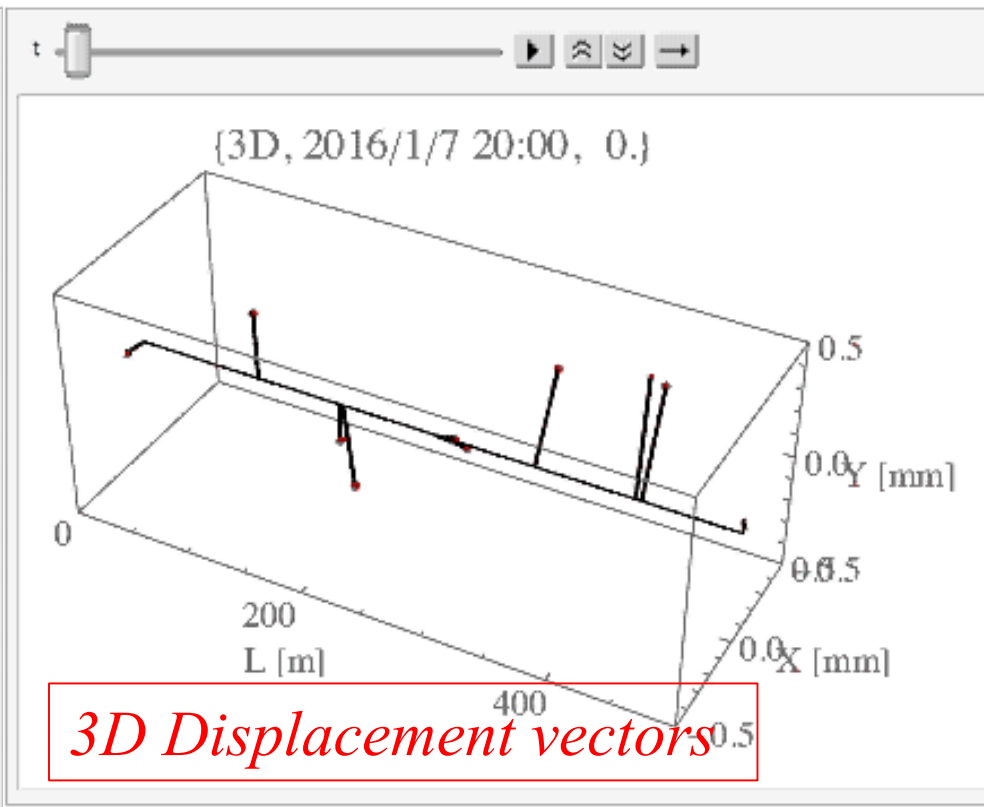
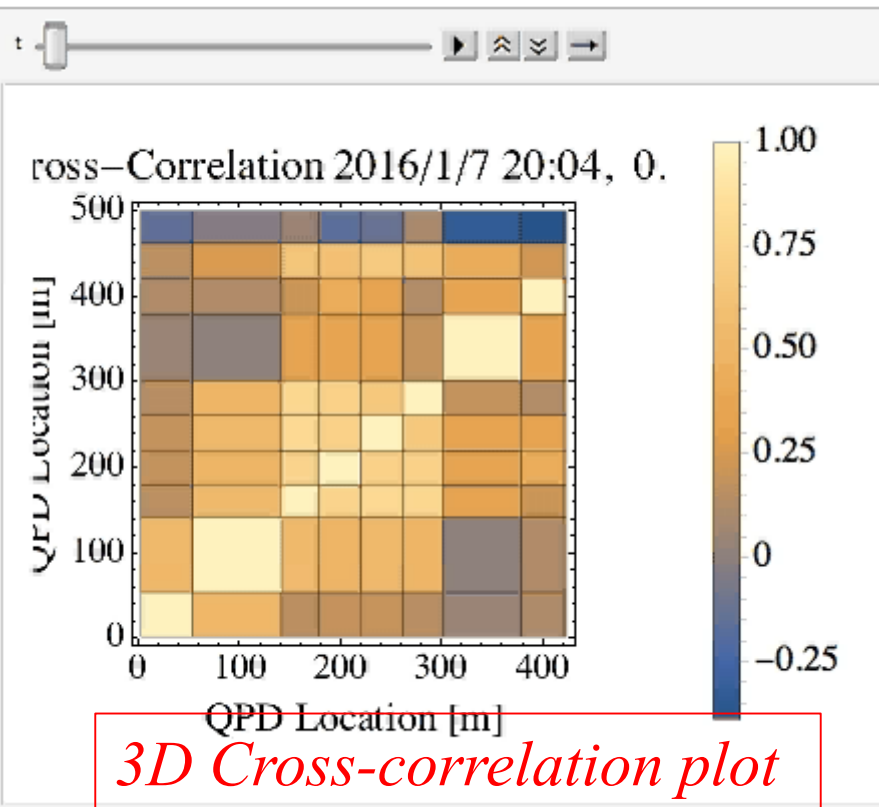
- (1) $\langle \mu(i) \rangle$: average of the n -th displacement vectors $d_n(i)$ of the i -th QPD in time series with a maximum data length of N .
- (2) $C_k(i, j)$: cross-covariance function between the n -th displacement vectors ($d_n(i)$ and $d_n(j)$) obtained for the i -th and j -th QPDs, respectively, in time series with time lag of k .
- (3) $R_k(i, j)$: cross-correlation function. $R_k(i, j)=1$ (-1) : strong positive (negative) correlation, $R_k(i, j)=0$: no correlation, $k=0$ ($k \neq 0$) stands for the cross-correlation function at present (past) time.

Cross-correlation analysis between the displacement vectors



- Time traces in the cross-correlation function of the displacement vectors between the reference QPD (QPD_REF28DA) and other QPDs for the accelerator units with the feedback control on during the same term.

Animations in time series for the cross-correlation analysis between the displacement vectors



Real-time measurement in time series of the cross-correlation function

Real-time measurement in time series of the displacement vector

Summary

- A new remote-controllable sensing system has been developed to measure slow dynamic displacements of the tunnel floor in real time at the KEKB injector linac.
- Based on the real-time measurements with the new system, we have observed non-negligible floor displacements due to dynamic ground motion during a half year period since 7 January 2016.
- The maximum norms in the displacement vector of the accelerator unit is 0.65 mm on average. The maximum growth rates is 5 $\mu\text{m}/\text{day}$ on average.
- It can be seen that the cross-correlation function varies irregularly and finely in the corresponding time trace, and however, the floor level in each building block moves coherently and integrally with each other on average along the entire length of the linac tunnel.
- We will install more remote-controllable QPDs by following a plan sequentially.

Back-up files

Time traces of the displacement vectors (cont'd)

- It can be understood that the norms of the displacement vectors monotonically increase (except for that of QPD REF1UA), while it can be seen that there are some incomprehensible fine structures in each time trace.
- The variations in the maximum norm (rm) of the displacement vector in each time trace as a function of the QPD location are spread over a range of 0.19-0.88 mm during a half year period, and the average maximum norm ($\langle rm \rangle$) is 0.65 mm.
- The variations in the maximum growth rates (sr) in the time traces as a function of the QPD location are spread over a range of 3.3-6.6 $\mu\text{m}/\text{day}$ depending on the QPD location, and the average maximum growth rate ($\langle sr \rangle$) is 4.9 $\mu\text{m}/\text{day}$.
- It can be clearly seen that relatively large stepwise jump arises on 28 January 2016 in the time traces of the phase for QPD_1814DA and QPD_28REFUA. It takes about four days in the rise time of the jump, and on the other hand, in the variations in the norms of the displacement vector during the corresponding term are less than 0.2 mm. It could be understood that during the corresponding term the displacement vector of the accelerator unit has rotated rather than increased in the transverse plane.

Cross-correlation analysis between the displacement vectors (cont'd)

- Each cross-correlation function varies *irregularly* in the corresponding time trace, and however, the averages in the time traces decrease **in the range of $R_0 = 0.67$ to 0.48** in accordance with the distance from the reference QPD (except for QPD REF1UA where $R_0 = 0.06$).
- Relatively strong positive cross-correlations show high coherency on average in dynamic displacements of the tunnel floor in the time series along the entire length of the linac tunnel (except for QPD REF1UA).
- It should be noted that the time trace in the cross-correlation function for QPD_REF1UA is markedly different from those in the other cross-correlation functions. It seems for QPD_REF1UA to stand alone from the other building blocks.

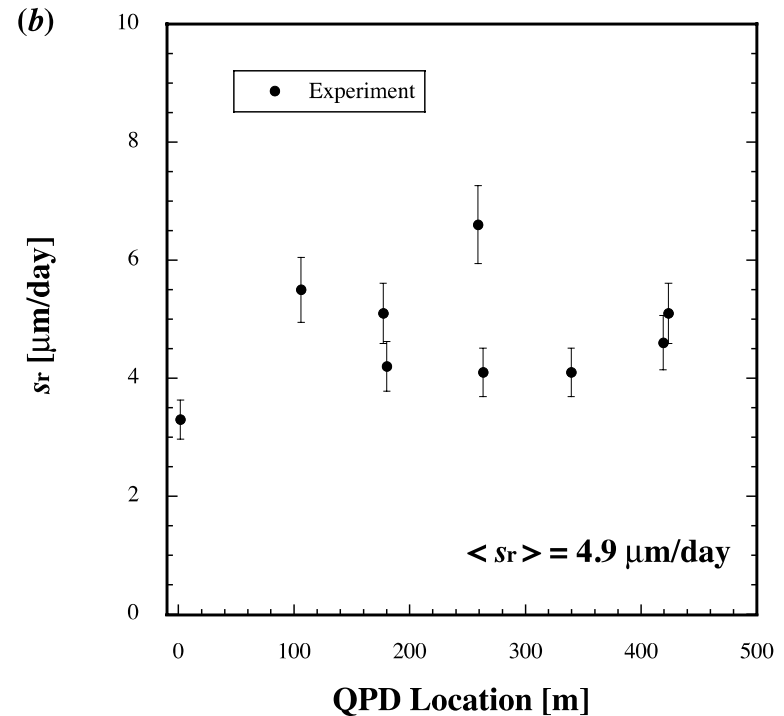
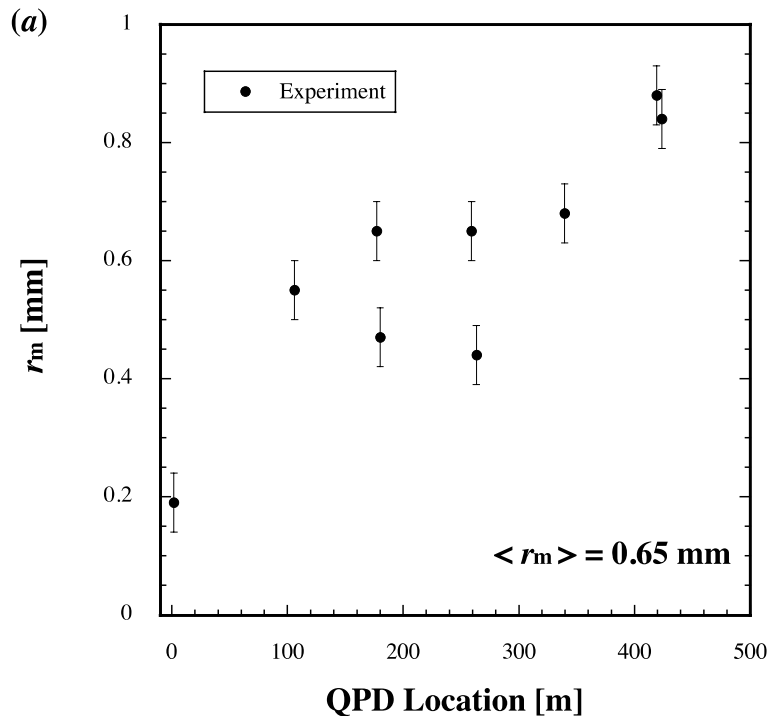
Cross-correlation analysis between the displacement vectors (cont'd)

- The 500-m-long linac building has two floors, which together constitute the klystron gallery and the in-ground tunnel.
- The linac building comprises eight building blocks that are joined to be linearly aligned with seven expansion joints, which can absorb a certain amount of elastic deformation caused by expansion or contraction of the building blocks.
- However, residual amounts of elastic deformation may induce deformation of the building blocks themselves. This may increase the displacement of the accelerator units through displacements of the tunnel floor, triggered by the complex processes that were mentioned previously.
- In particular, it should be noted that the fiducial points created by the laser axis can move dynamically and independently in proportion to the displacement vector of the tunnel floor, even though the last fiducial point is strictly fixed at the last QPD center with the feedback control on.
- Therefore, the laser axis itself cannot become an entirely fixed and stable fiducial axis as an absolute fiducial line, because it is not possible to directly stabilize dynamic ground motion.

Data-taking procedure in the real-time measurement

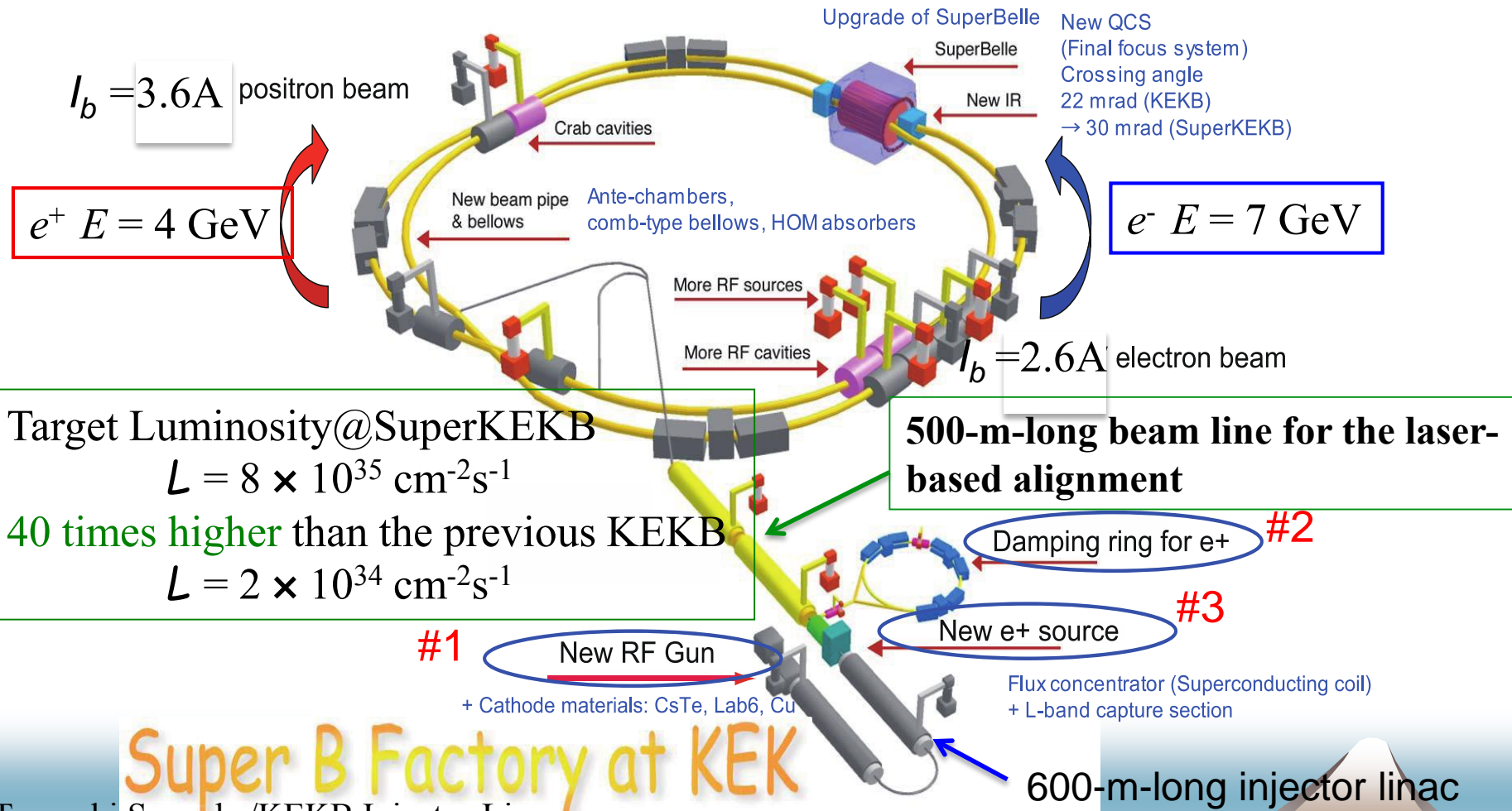
- Every four hours on the hour, the basic functions provided by the server start to work in order to take a series of the displacement data for all the QPDs.
- The basic functions comprise
 - *a) feedback control for the laser axis*, the end positions of the laser axis at the last QPD are stabilized by the feedback control until the transverse positions of the laser axis are within the allowable region of $\pm 50 \mu\text{m}$ from the center of the last QPD.
 - *b) actuator control for the QPD*, the first upstream QPD is driven to the central position of the laser pipe.
 - *c) data taking for the QPD*, displacement data of the QPD are repeatedly taken one thousand times, then average and standard deviation are calculated by using the four output voltages along with the x and y displacements.

Real-time measurements on dynamic floor motion



- Variations of (a) the maximum norm and (b) the maximum growth rate in the displacement vector measurements as a function of the QPD location.

The Super KEKB : an electron-positron collider with asymmetric energies



Target Luminosity@SuperKEKB

$$L = 8 \times 10^{35} \text{ cm}^{-2}\text{s}^{-1}$$

40 times higher than the previous KEKB

$$L = 2 \times 10^{34} \text{ cm}^{-2}\text{s}^{-1}$$

Super B Factory at KEK

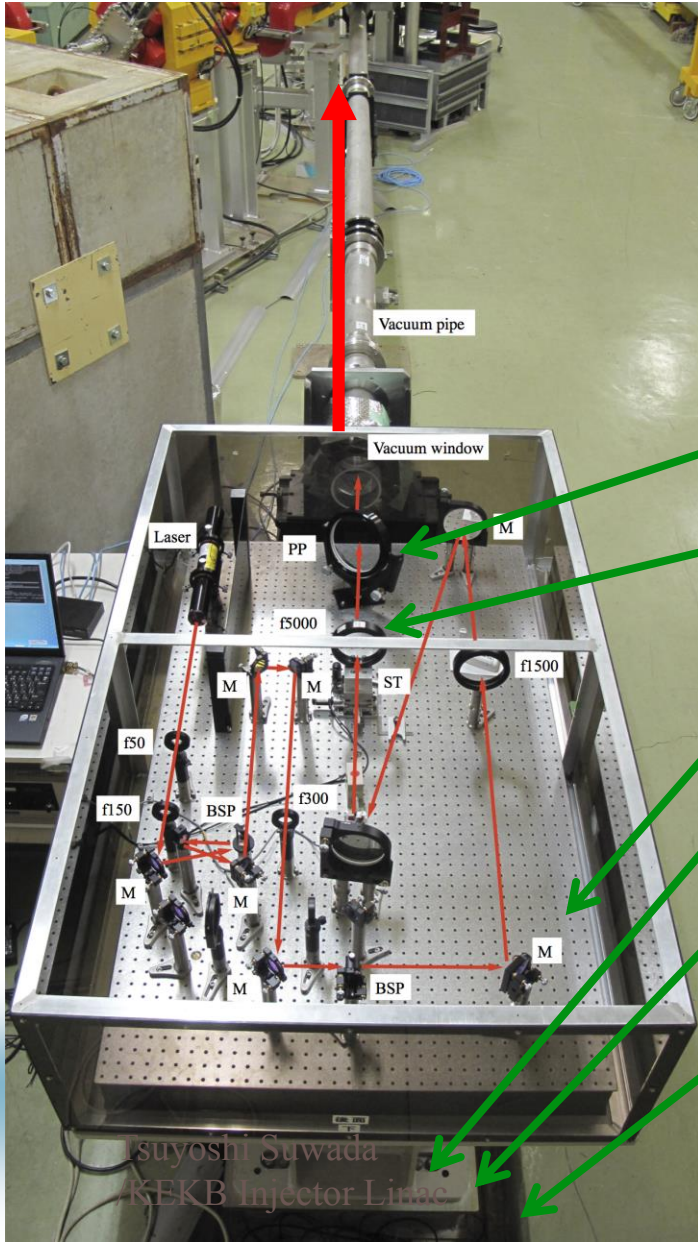
Tsuyoshi Suwada /KEKB Injector Linac

Tsuyoshi Suwada

/KEKB Injector Linac

IWAA2016, 3-7 Oct., 2016 @ ESRF, Grenoble, France

Injection Optical System



Optical system

- 10-mW He-Ne laser
- Solid and large optical table

Vacuum system

- Two scroll pumps (1000l/min)
- Vacuum level ~ 3 [Pa]

Parallel plate for translation tuning

f5000 lens for injection angle tuning

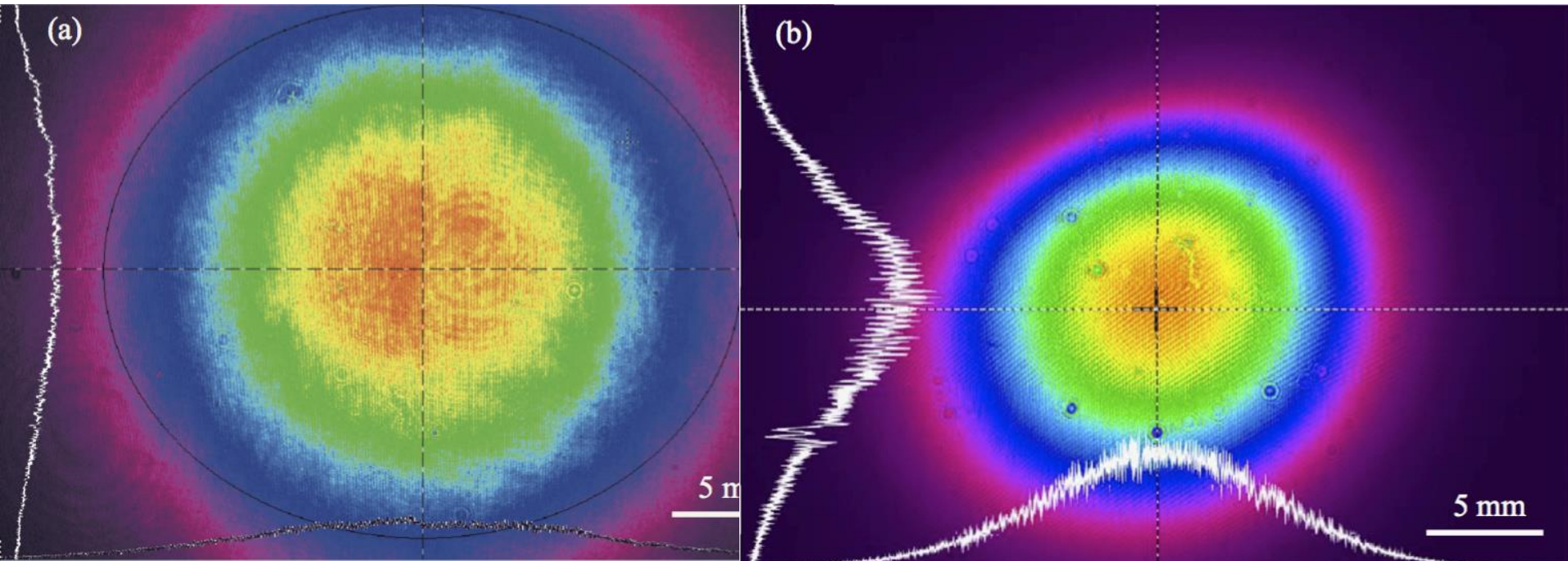
Optical table (1500×900×112^tmm³)

Girder (Fe)

Iron plate (1510×500×20^tmm³)

Isolated floor separated from the tunnel floor by a 100-mm gap (1510×500mm²)

Laser profiles at the initial and last QPDs



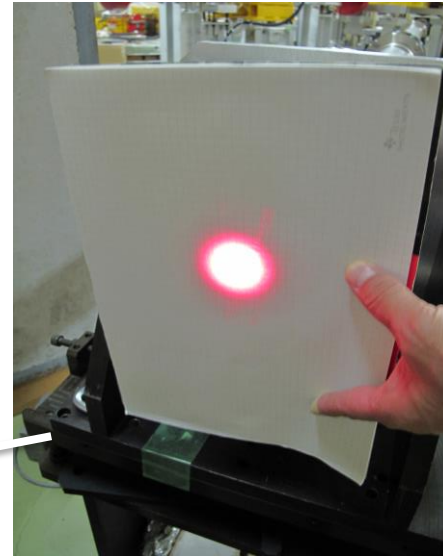
@ Exit of the optical system ($z=0$)
 $W_x \approx W_y \approx 29\text{mm}$ (4σ width)

@ Last QPD ($z=500\text{m}$)
 $W_x \approx 21.2\text{mm}$ (4σ width)
 $W_y \approx 17.8\text{mm}$

10-mW He-Ne Laser delivering

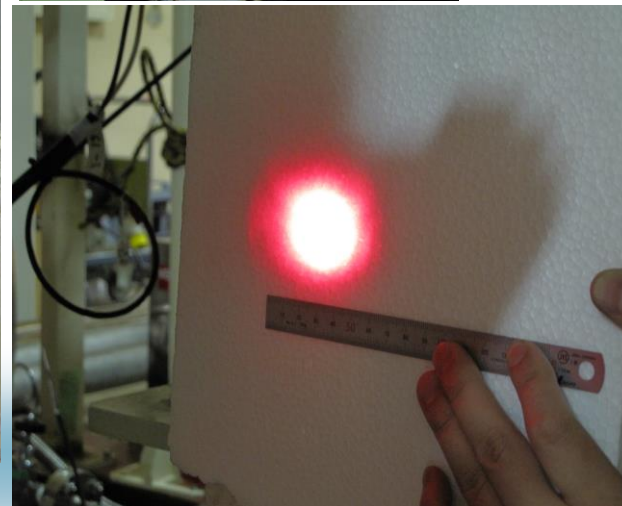


Vacuum level $\sim 5\text{Pa}$ in laser pipes
with two scroll pumps (1000l/min)

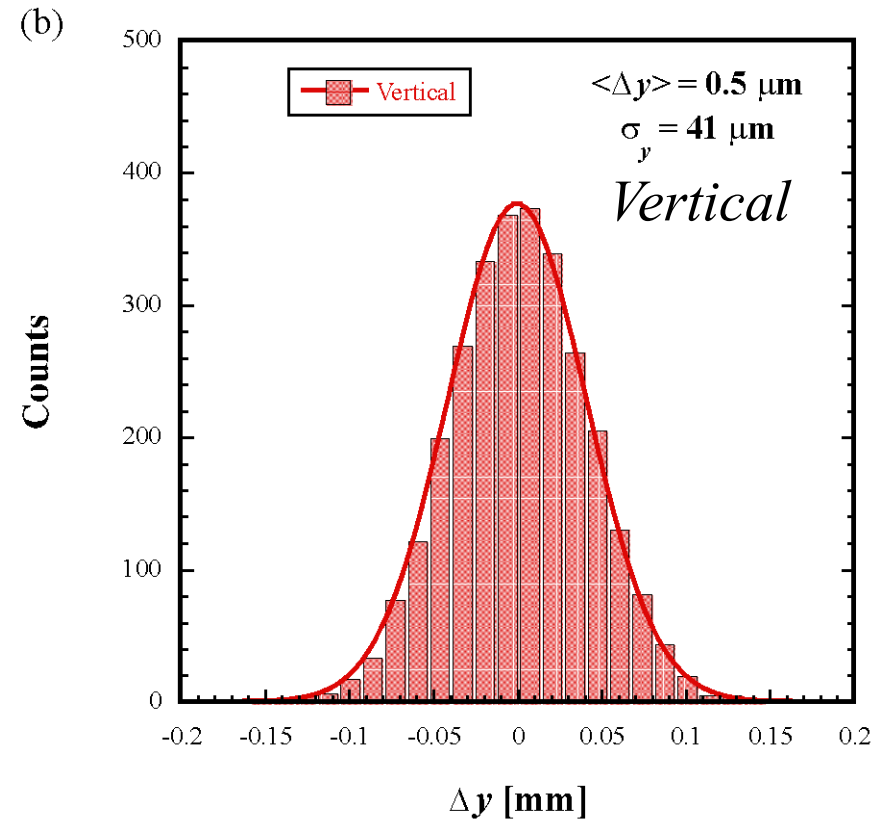
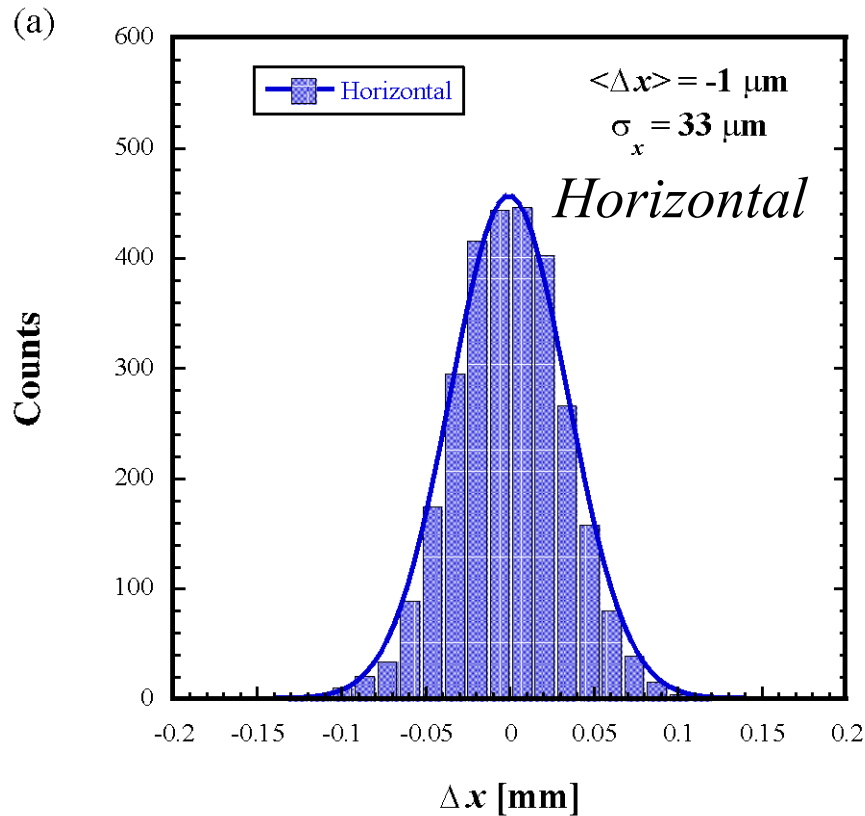


W $\sim 30\text{mm}$ (FW)
at the injection point

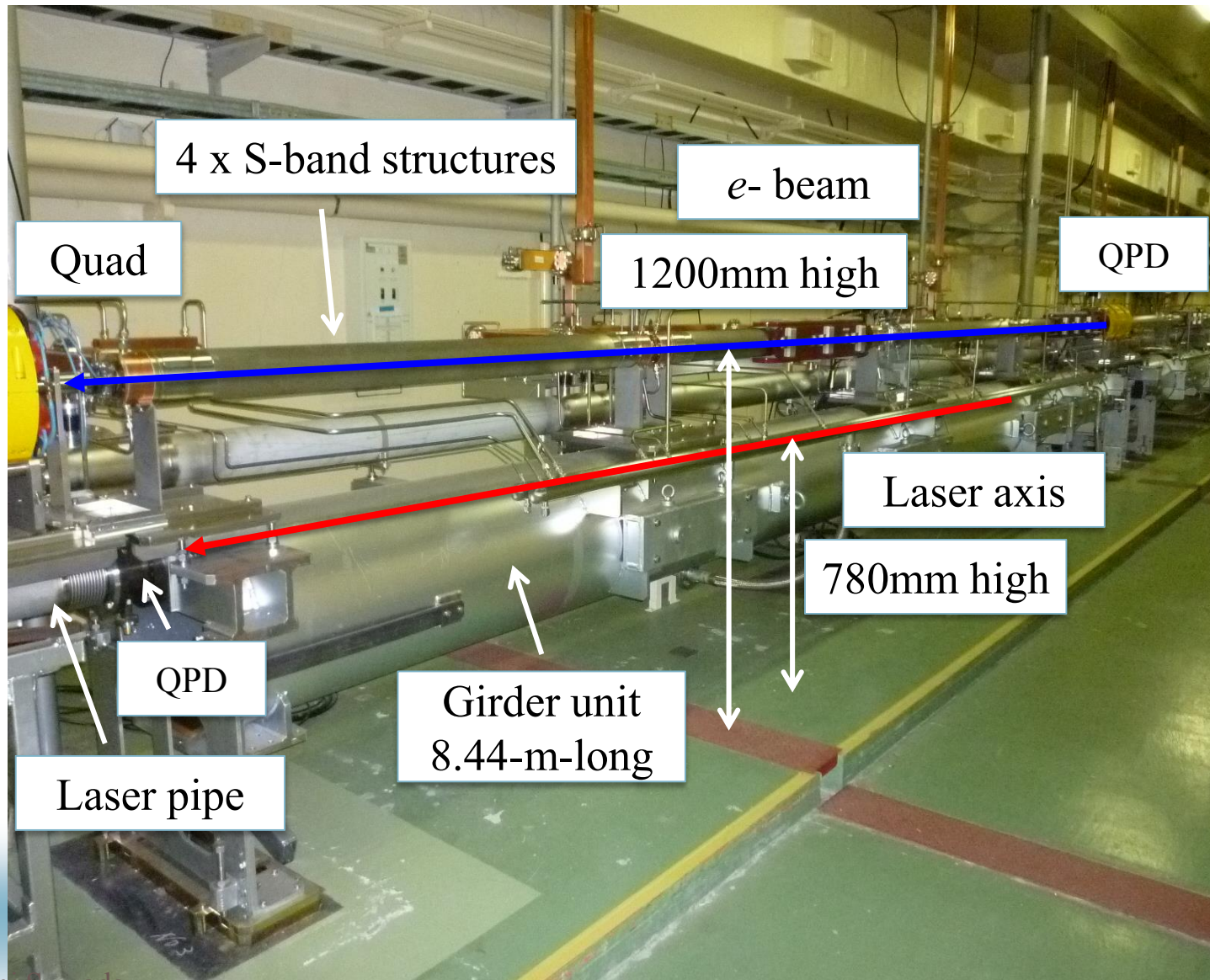
W $\sim 30\text{mm}$ (FW)
at the 500m-long linac
end point



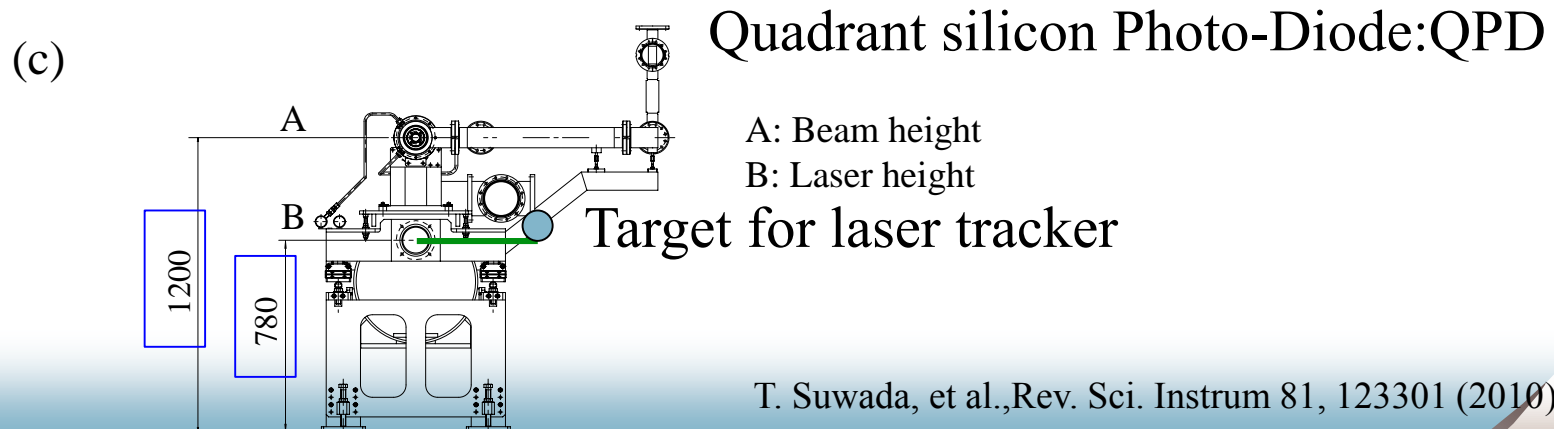
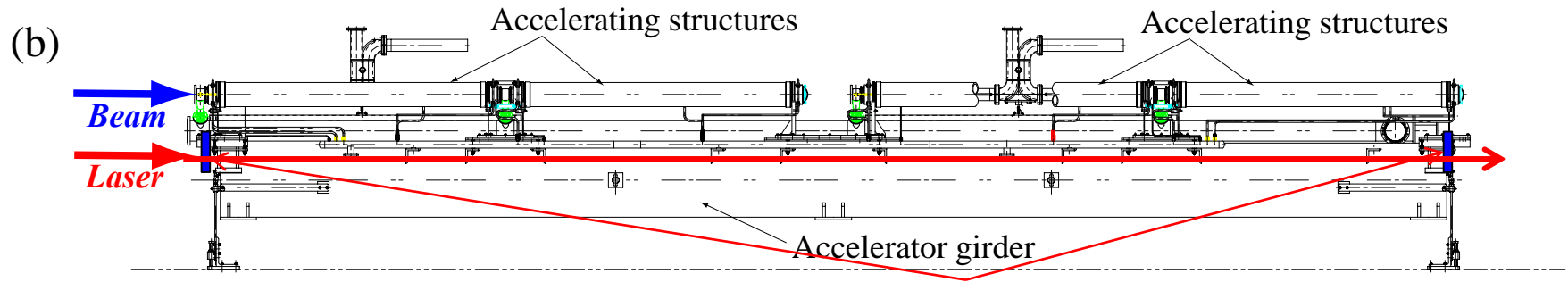
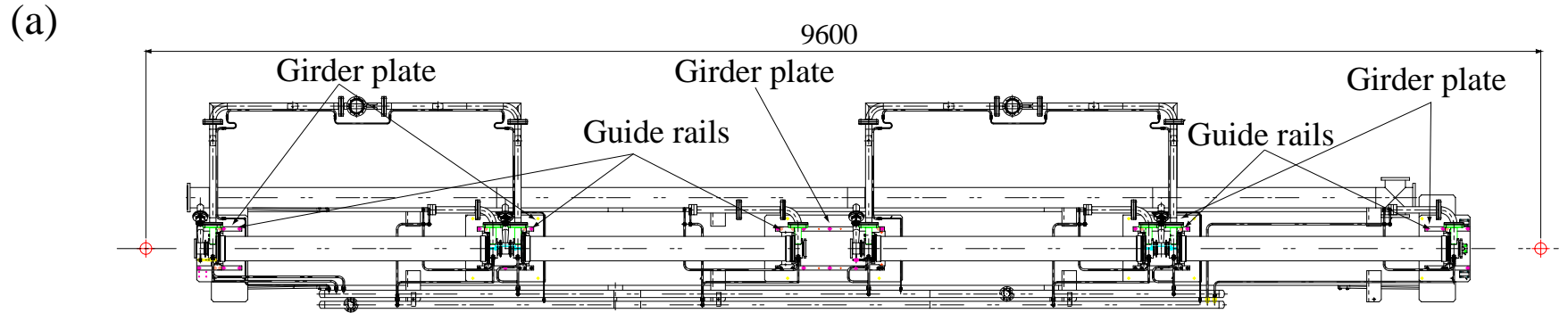
Position displacement distributions of the laser axes for 500-m-long straight line



Girder unit for accelerating structures

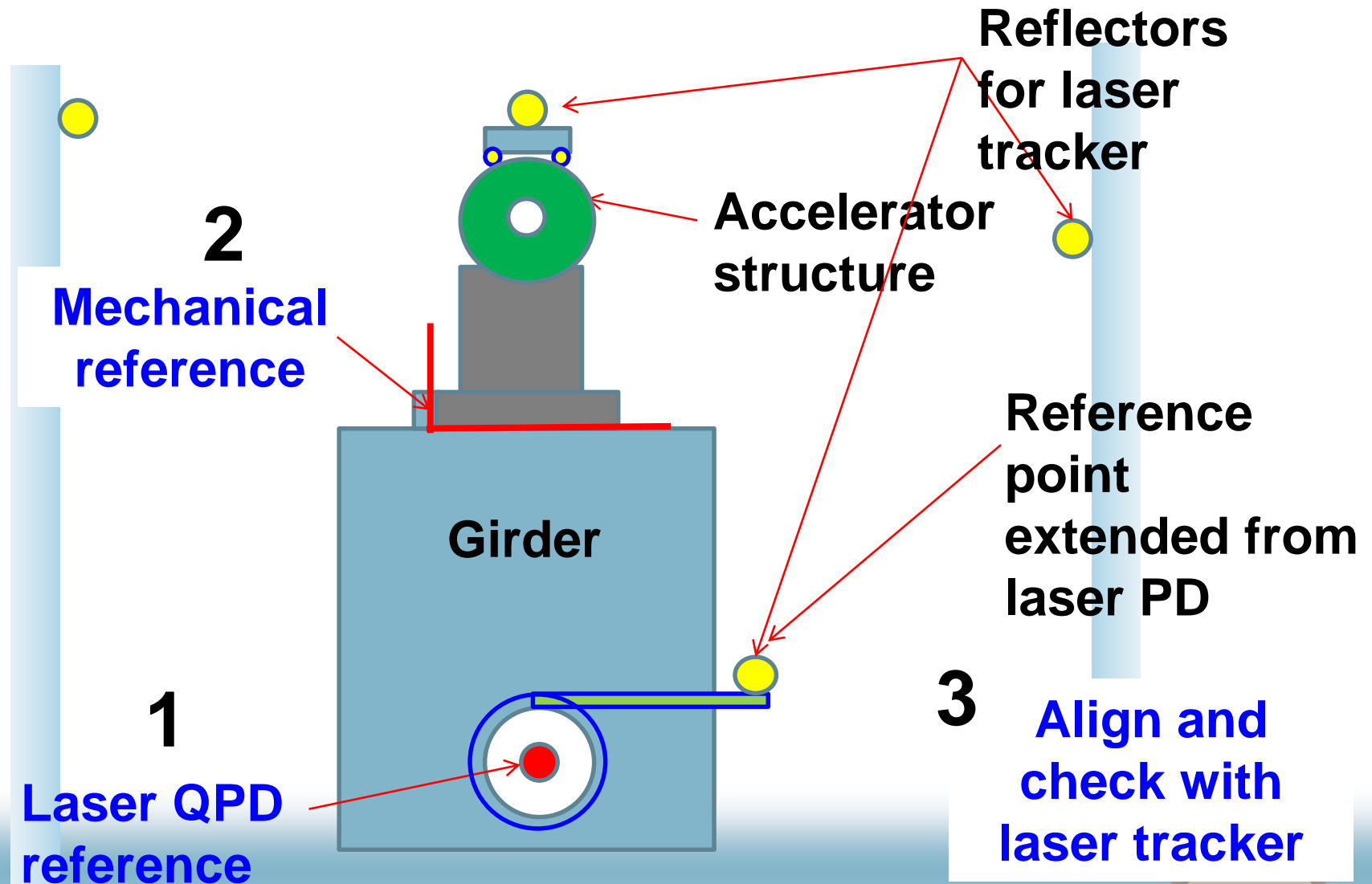


Girder unit structure

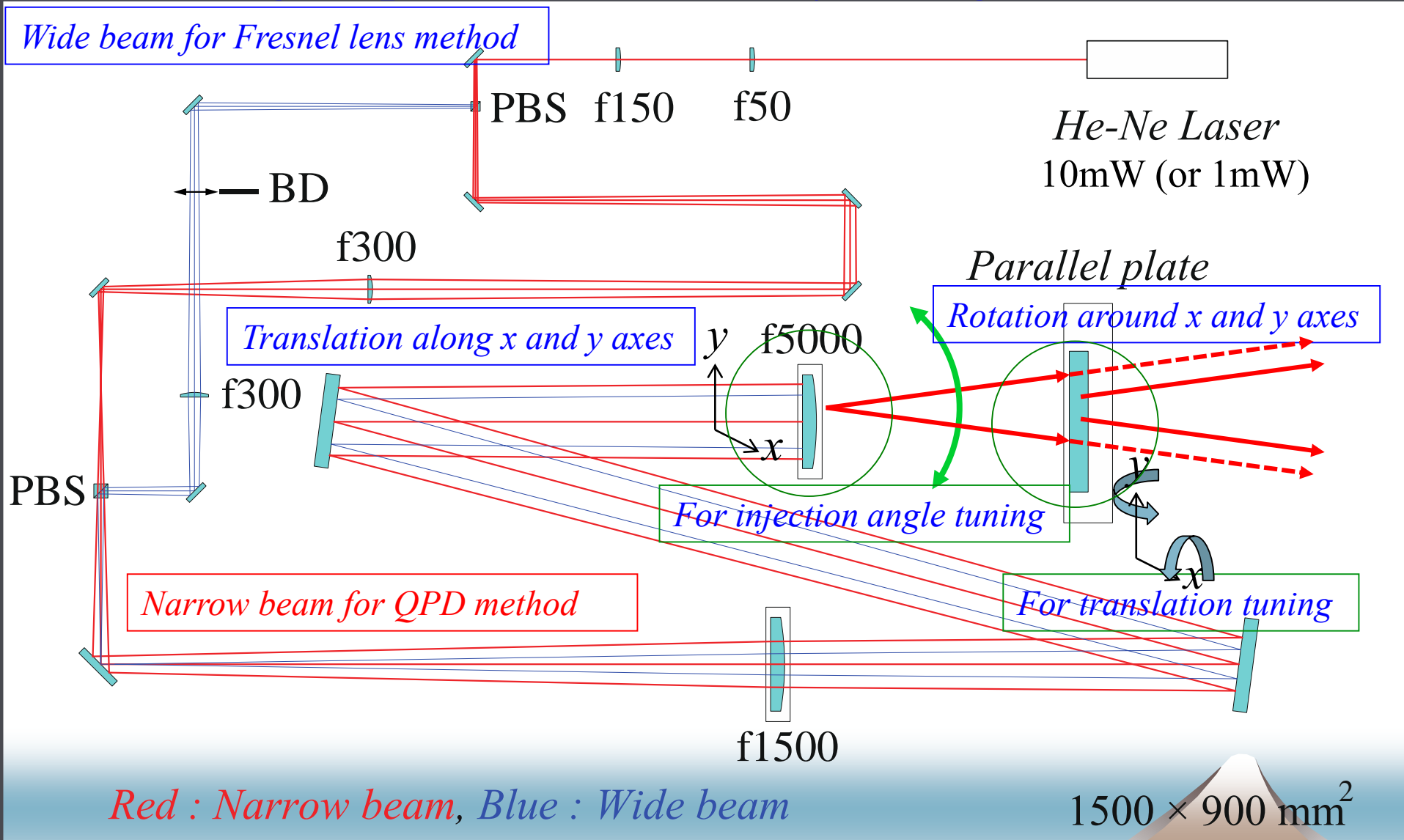


T. Suwada, et al., Rev. Sci. Instrum 81, 123301 (2010).

Short range component alignment on the girder



Laser optical system – simple dioptric system using dioptric lenses and reflecting mirrors –



QPD Tests on radiation hardness

PD /r. r. (%)	1 st . (Apr/26-May/19)	2 nd . (Apr/26-June/02)	3 rd . (Apr/26-June/16)	4 th . (Apr/26-June/30)
O 社 PD Ch1	7.5	1.9	4.8	34
Ch2	8.5	1.5	0.67	28
Ch3	3.7	-5.1	12	28
Ch4	5.7	4.9	8.6	35
S1227-66BR	0.28	0.84	0.14	5.6
S5106	8.0	12.	18	95

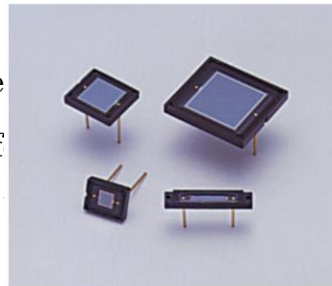
Present QPD,
OSI (SPOT-9D)

Hamamatsu
~6 times rad.
hard

Table.1 Test results of radiation hardness for several QPD samples at the KEKB injector linac.
The value is indicated by the reduction rate (r. r.%) of the output voltage before radiation exposure to that after radiation exposure.

The samples for the 1st, 2nd, and 3rd measure positron separator, and however, the samples for positron target. All the samples were exposed under nominal operation condition.

HAMAMATSU
PHOTON IS OUR BUSINESS



Siフォトダイオード

S1227シリーズ

紫外～可視域精密測光用、赤外感度抑制タイプの
フォトダイオード

Cross-correlation analysis between the displacement vectors

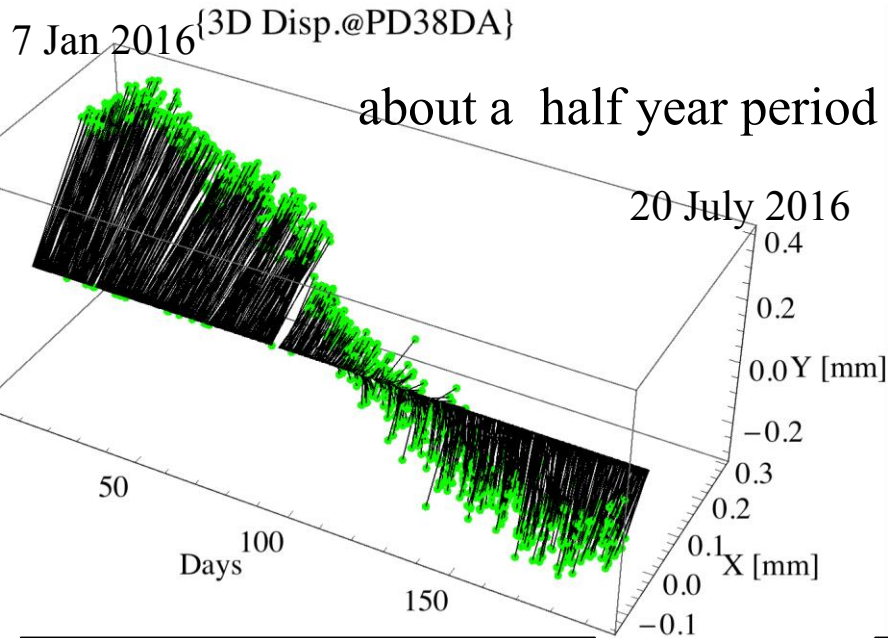
$$\langle \vec{\mu}(i) \rangle = \frac{1}{N} \sum_{n=1}^N \vec{d}_n(i), \quad (1)$$

$$\hat{C}_k(i, j) = \frac{1}{N} \sum_{n=1}^N (\vec{d}_n(i) - \langle \vec{\mu}(i) \rangle) \cdot (\vec{d}_{n-k}(j) - \langle \vec{\mu}(j) \rangle), \quad (2)$$

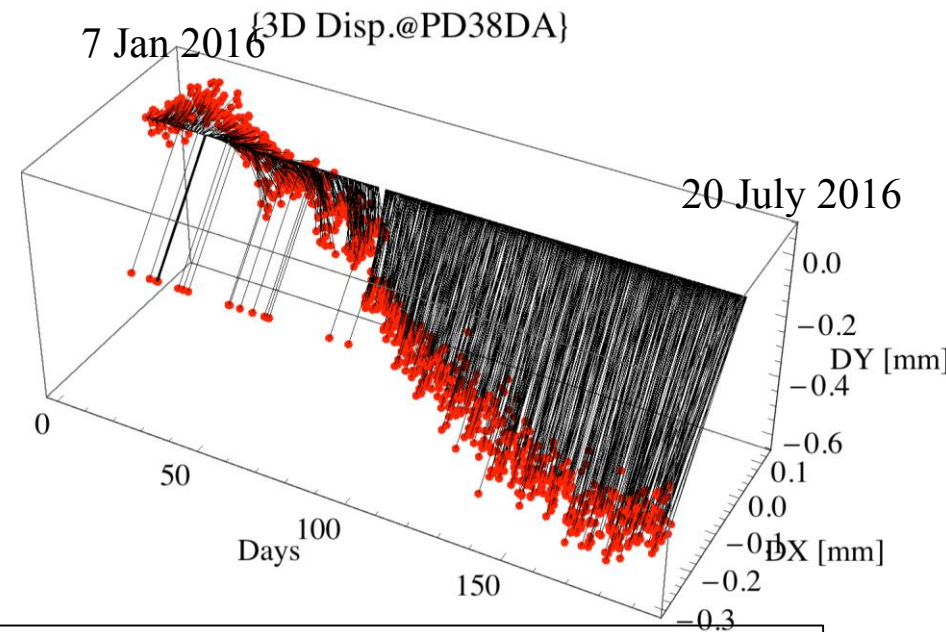
$$\hat{R}_k(i, j) = \frac{\hat{C}_k(i, j)}{\sqrt{\hat{C}_0(i, i) \hat{C}_0(j, j)}}. \quad (3)$$

- (1) $\langle \mu(i) \rangle$: average of the n -th displacement vectors $d_n(i)$ of the i -th QPD in time series with a maximum data length of N .
- (2) $C_k(i, j)$: cross-covariance function between the n -th displacement vectors ($d_n(i)$ and $d_n(j)$) obtained for the i -th and j -th QPDs, respectively, in time series with time lag of k .
- (3) $R_k(i, j)$: cross-correlation function. $R_k(i, j)=1$ (-1) : strong positive (negative) correlation, $R_k(i, j)=0$: no correlation, $k=0$ ($k \neq 0$) stands for the cross-correlation function at present (past) time.

Typical displacement vectors @ QPD-38DA



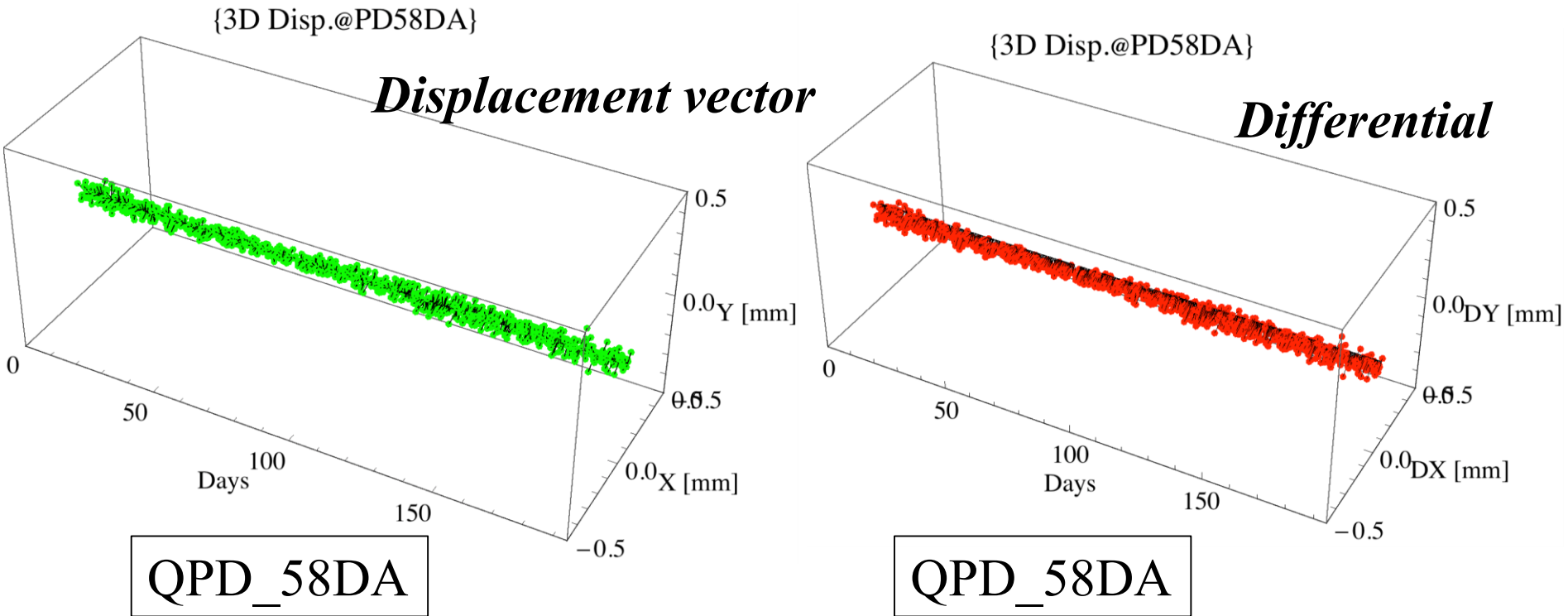
displacement vector



differential displacement vector

- Every four hours on the hour, the basic functions provided by the server start to work in order to take a series of the displacement data for all the QPDs.
- The results show typical variations in a time trace of the displacement vector obtained for the accelerator units with the feedback control on.
- It can be seen that the displacement vector has complicatedly rotated around the laser axis along with the growth of the vector norm in the time direction.

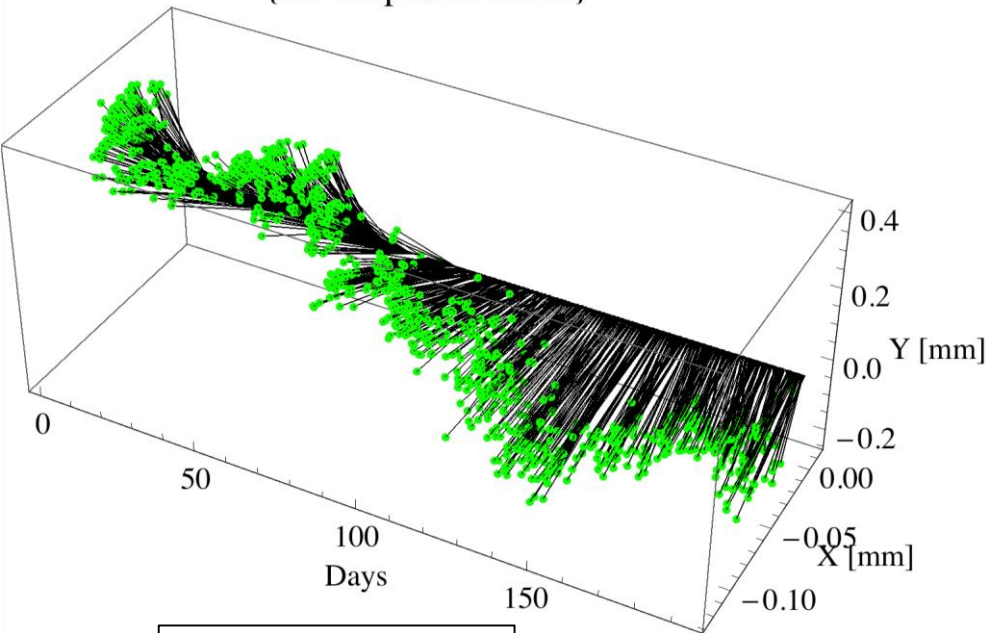
Introduction of the Displacement vectors



- Variations in a time trace of the displacement vector obtained for the QPD_58DA which is a feed-backed reference.

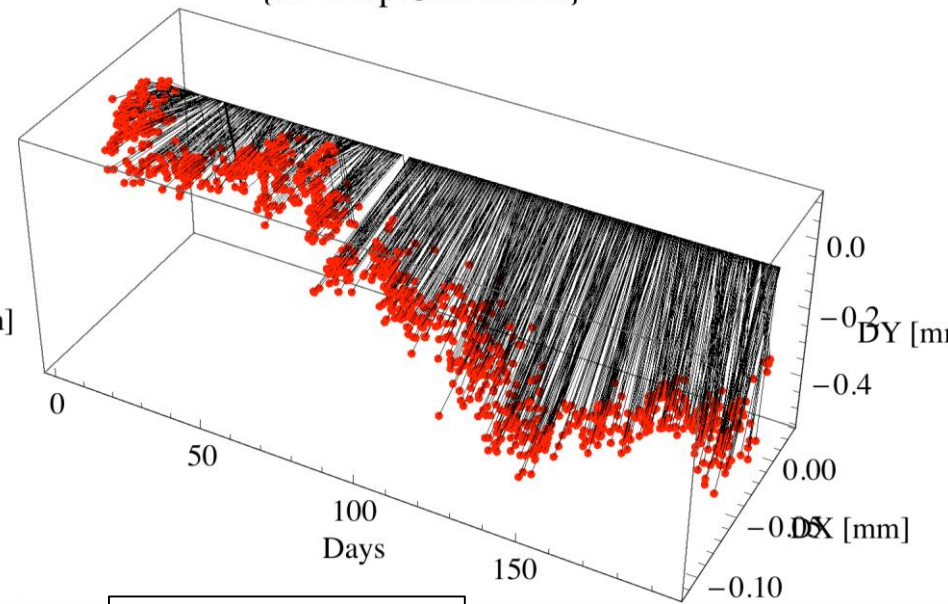
Introduction of the Displacement vectors

{3D Disp.@PD11DA}



QPD_11DA

{3D Disp.@PD11DA}



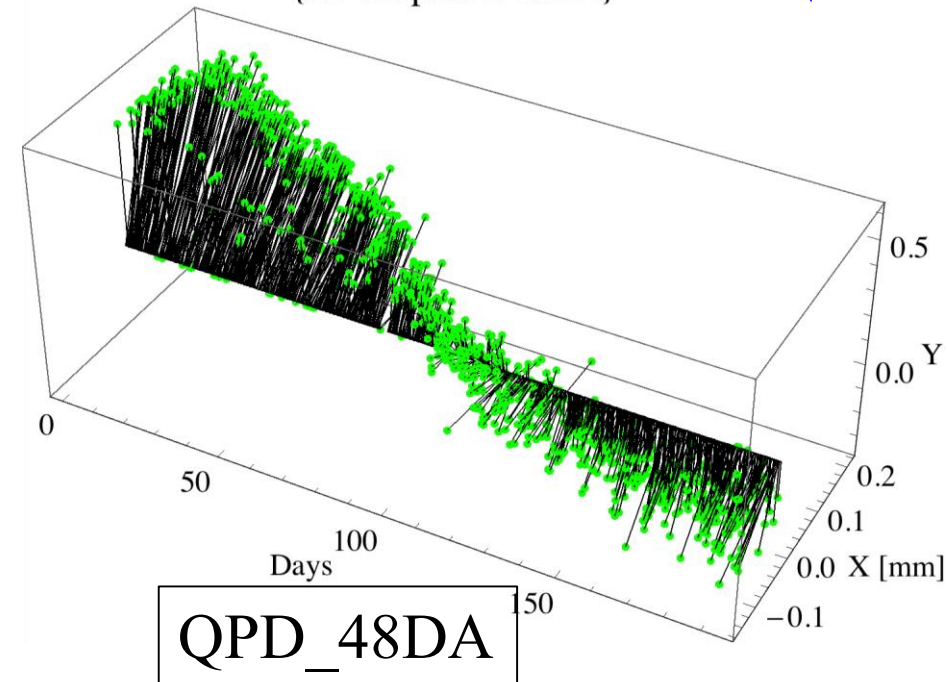
QPD_11DA

- Variations in a time trace of the displacement vector obtained for the accelerator units with the feedback control on.
- It can be seen that the displacement vector has complicatedly rotated around the laser axis along with the growth of the vector norm in the time direction.

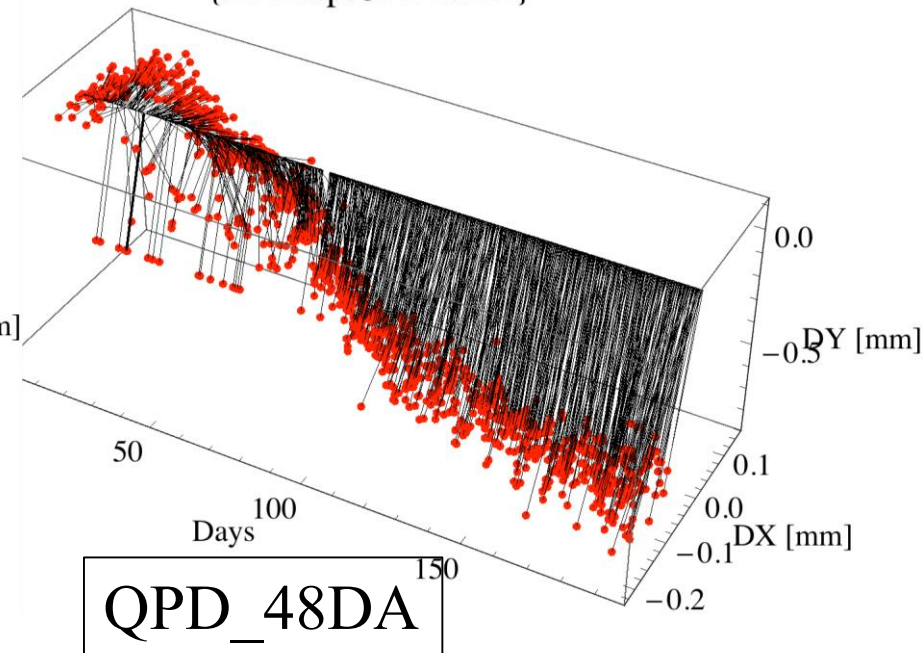
Introduction of the Displacement vectors

(cont'd)

{3D Disp.@PD48DA}



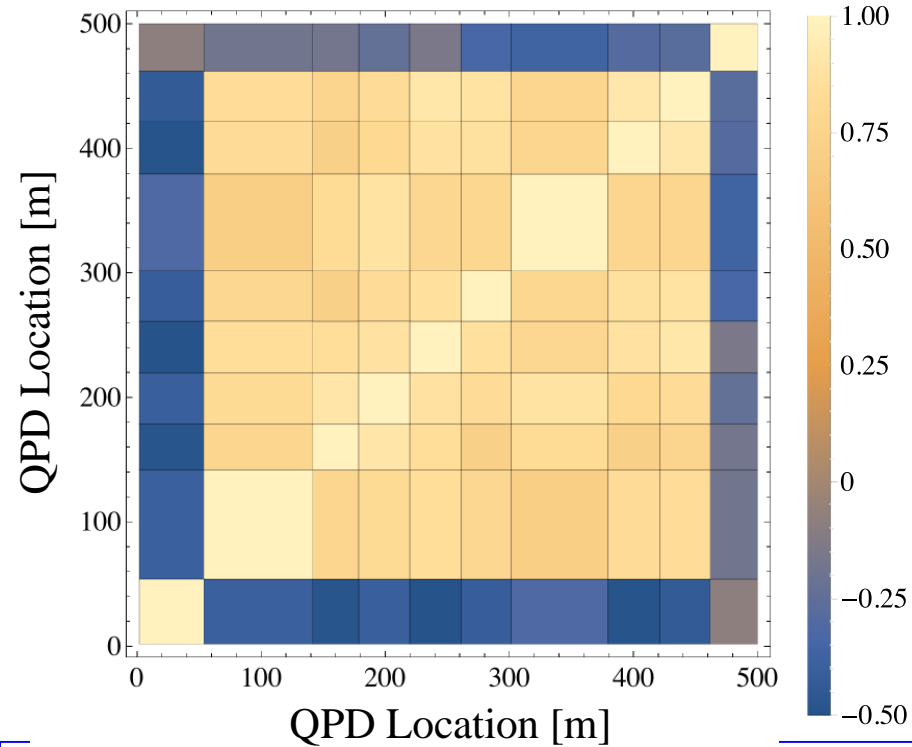
{3D Disp.@PD48DA}



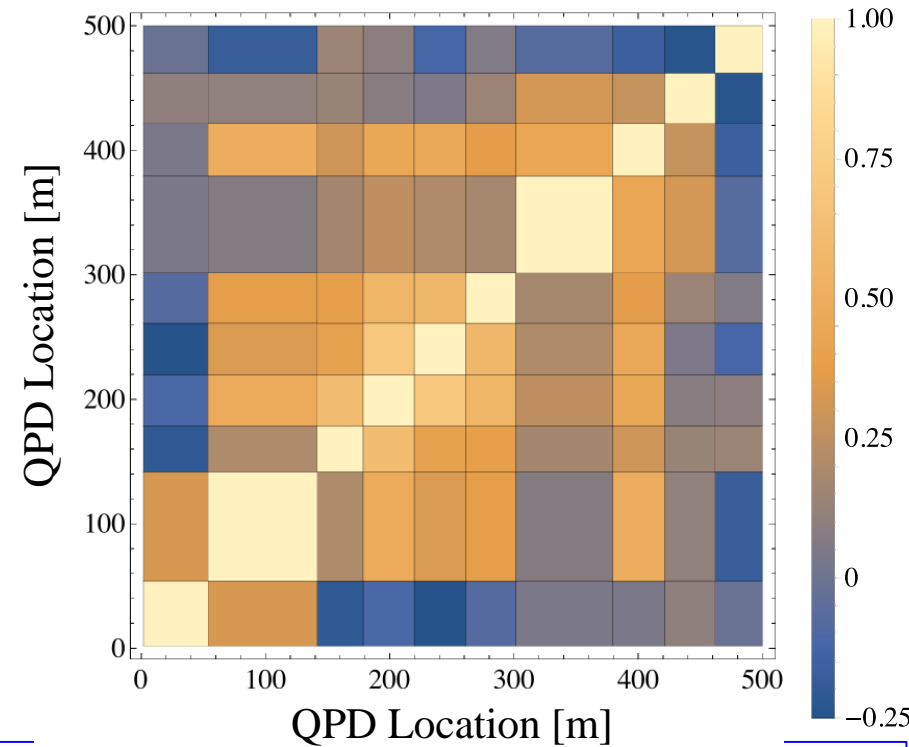
- Variations in a time trace of the differential displacement vector obtained for the accelerator units with the feedback control on.
- It can be seen that the displacement vector has complicatedly rotated around the laser axis along with the growth of the vector norm in the time direction.

Cross-correlation analysis between the displacement vectors (cont'd)

(a)



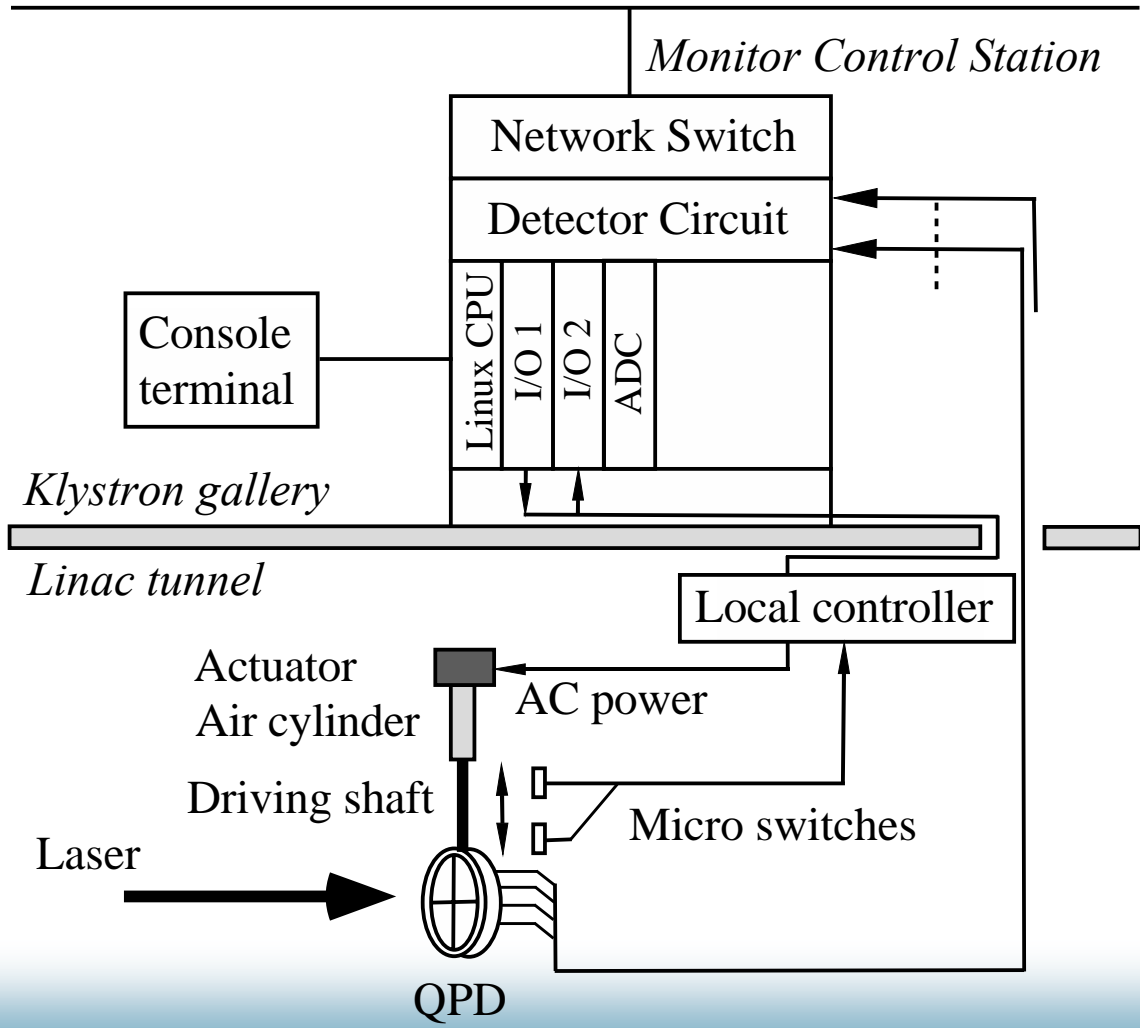
(b)



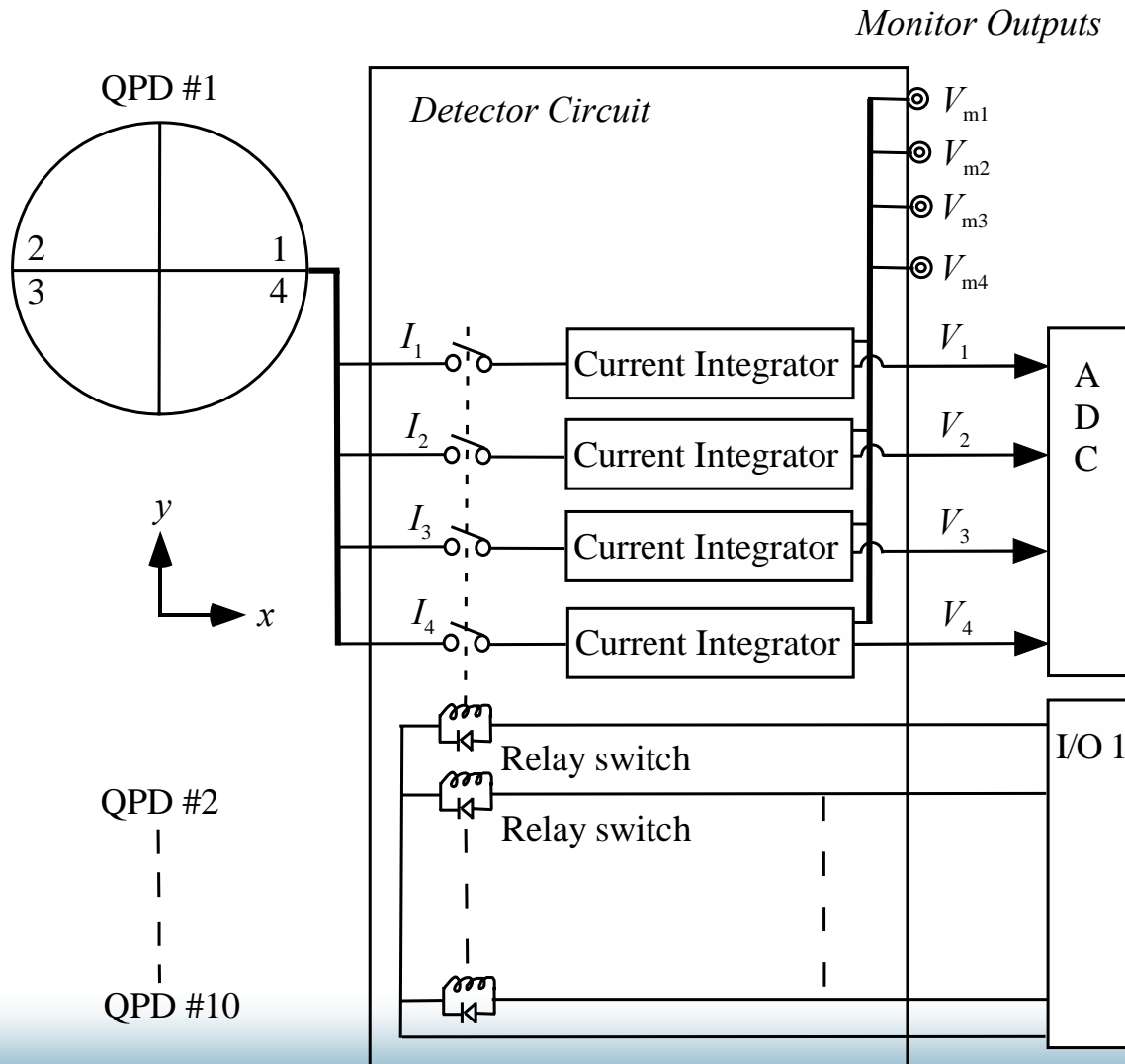
- Intensity distributions in the cross-correlation function between all the QPDs in the displacement vector measurements of the accelerator units along the C5 straight section obtained on (a) 15 February 2016 at 0:00 am and (b) 27 February 2016 at 8:00 am. The intensity distribution pattern in the cross-correlation function is linearly encoded by the color scale.

Block diagram of a local control system

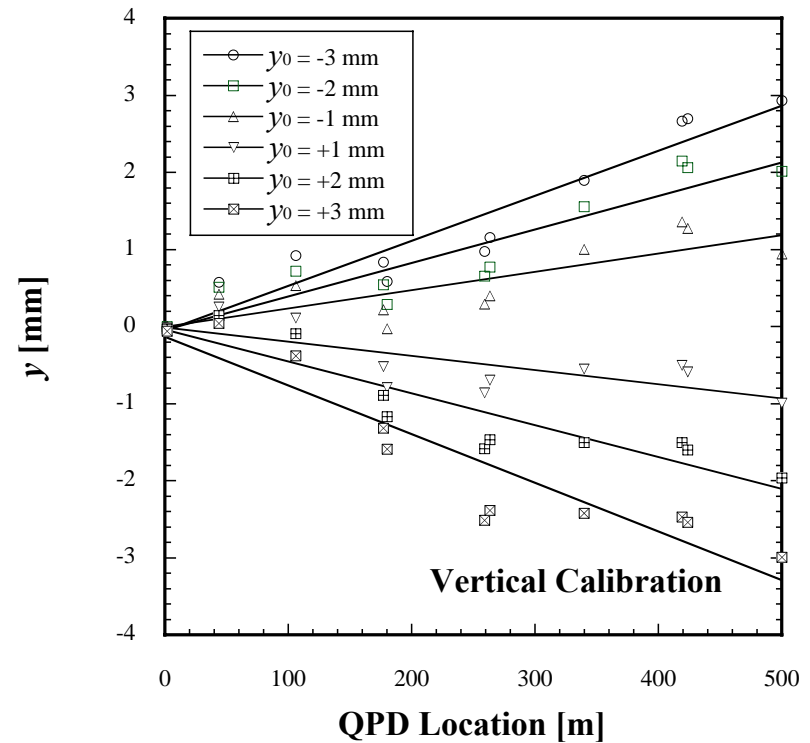
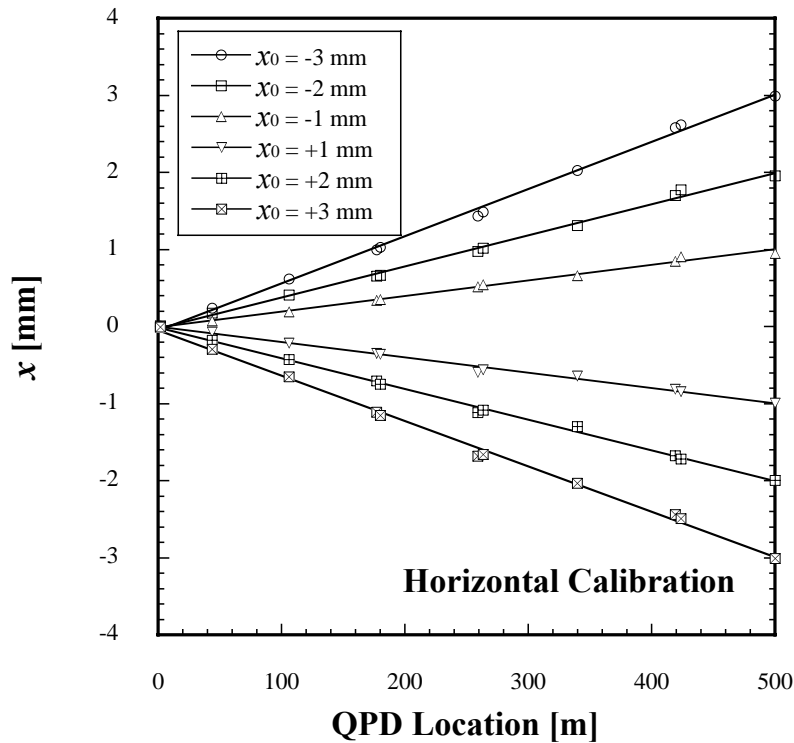
Linac control network



Detector circuit in the local control system



Calibration procedure for the QPD displacement to the laser axis

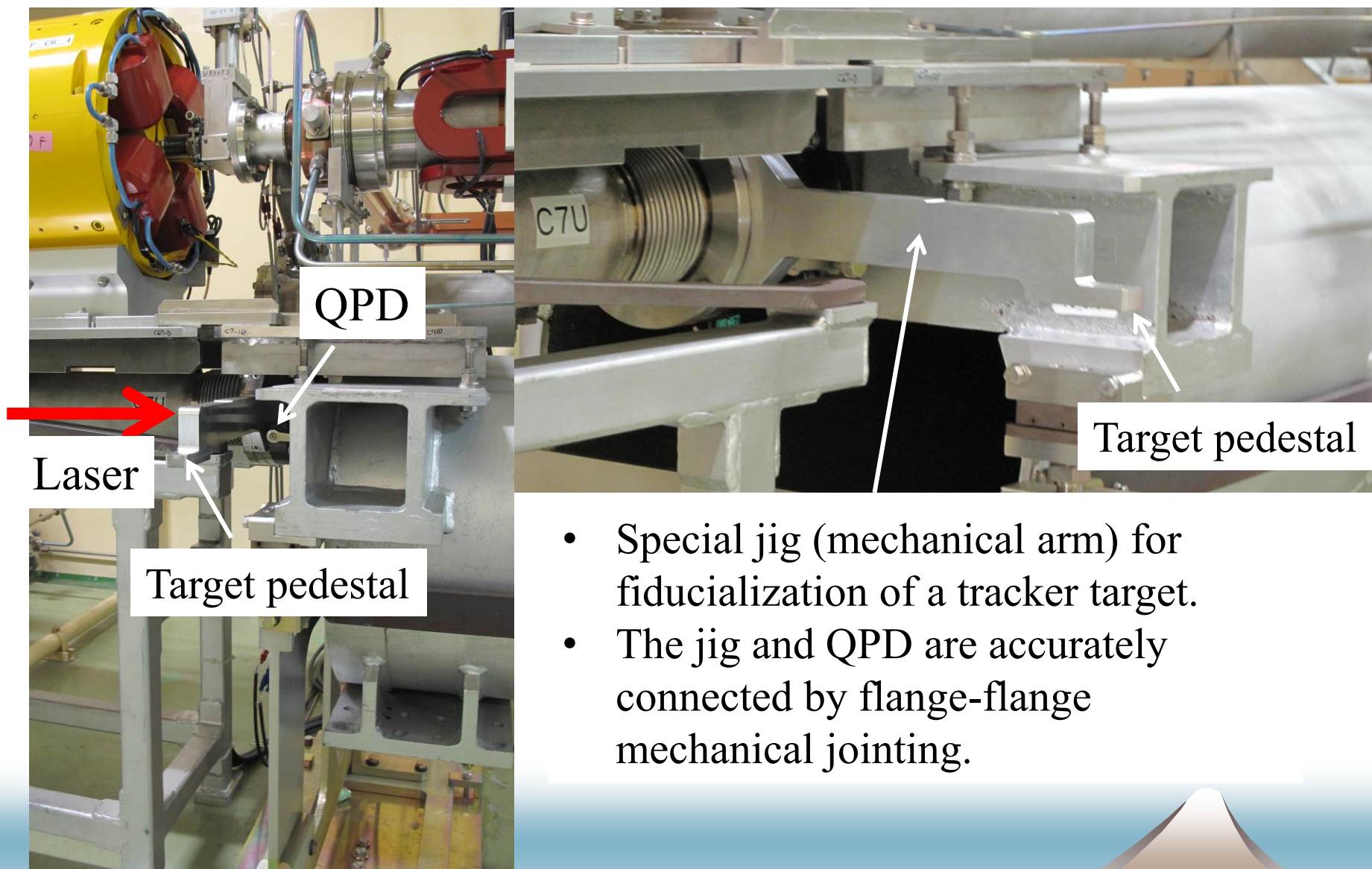


- Results in the horizontal calibration procedure for all the remote-controllable QPDs. It should be noted that a laser source and the fiducial QPDs are located at $z = 0$ and $z = 500$ m, respectively. The target positions controlled with the feedback control are defined by x_0 and y_0 at $z = 500$ m.

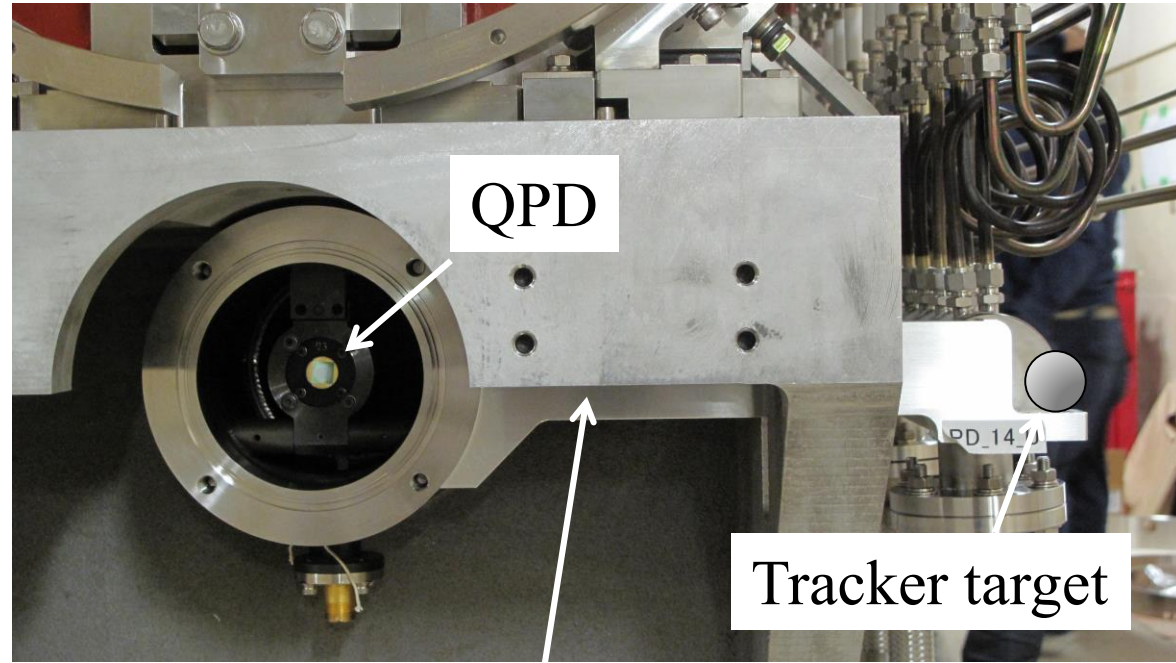
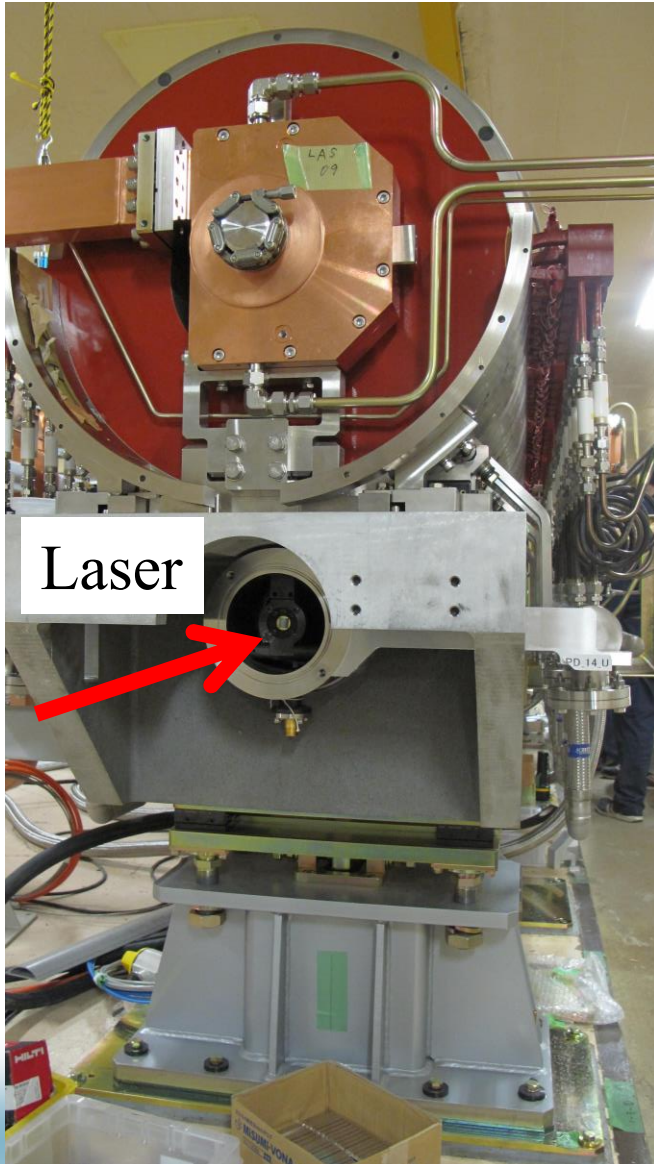
Laser size measurements along the linac

- The beam widths were directly measured at the two fiducial points ($z=0$ and $z=500\text{m}$).
- At other locations, they were analyzed by taking mapping data obtained with the help of mechanically movable QPDs while the laser beam was fixed. The mapping data were obtained by measuring the variations in the signal levels obtained from the QPD depending on the transverse displacements with respect to the fiducial line.
- The beam widths were analyzed by a least-square fitting procedure with a two-dimensional Gaussian function for the obtained mapping data.

Reference target for component alignment on the girder



Component alignment on the girder



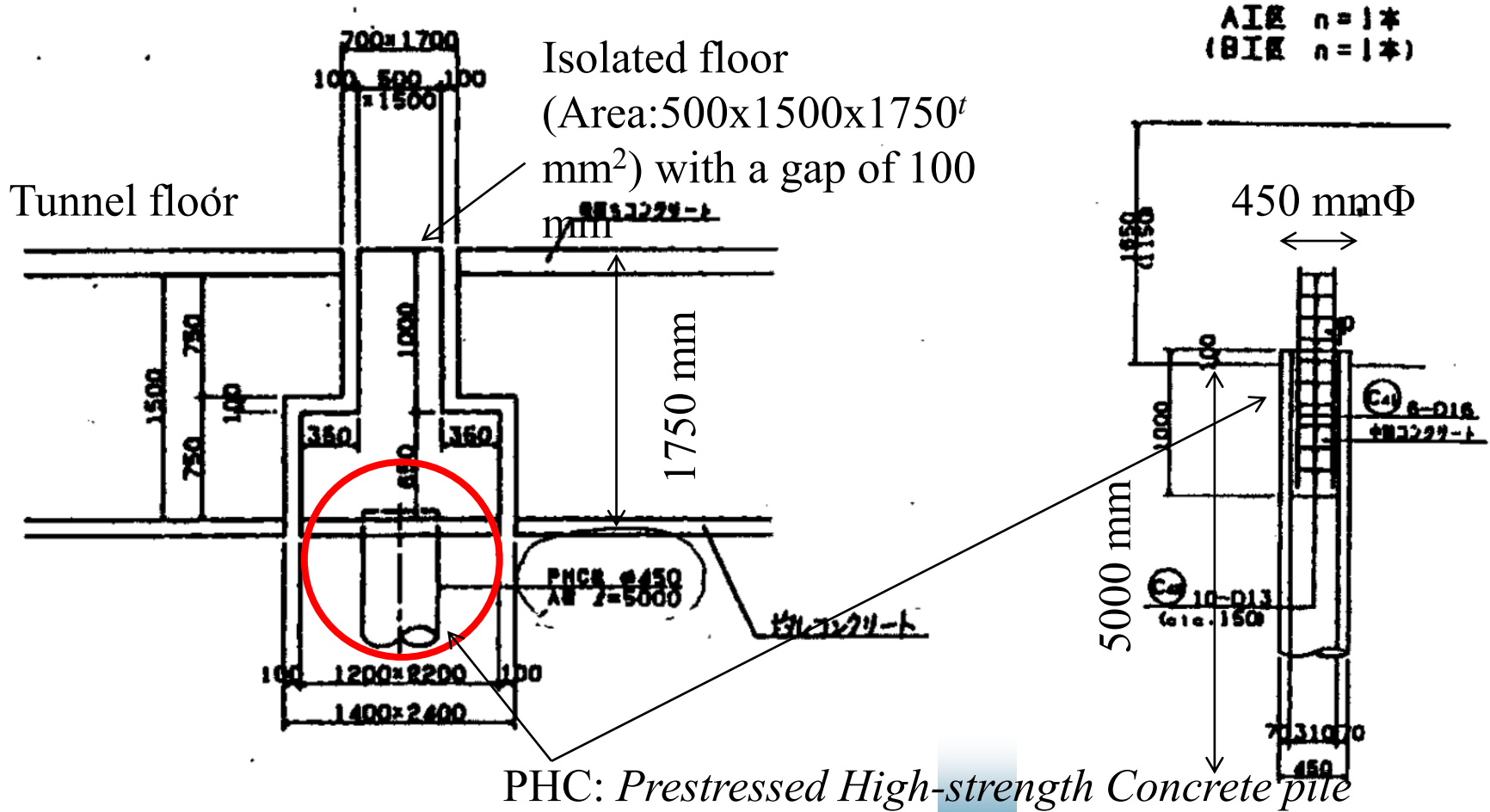
Special jig for fiducialization of tracker target

Isolated floor structure at the optical system

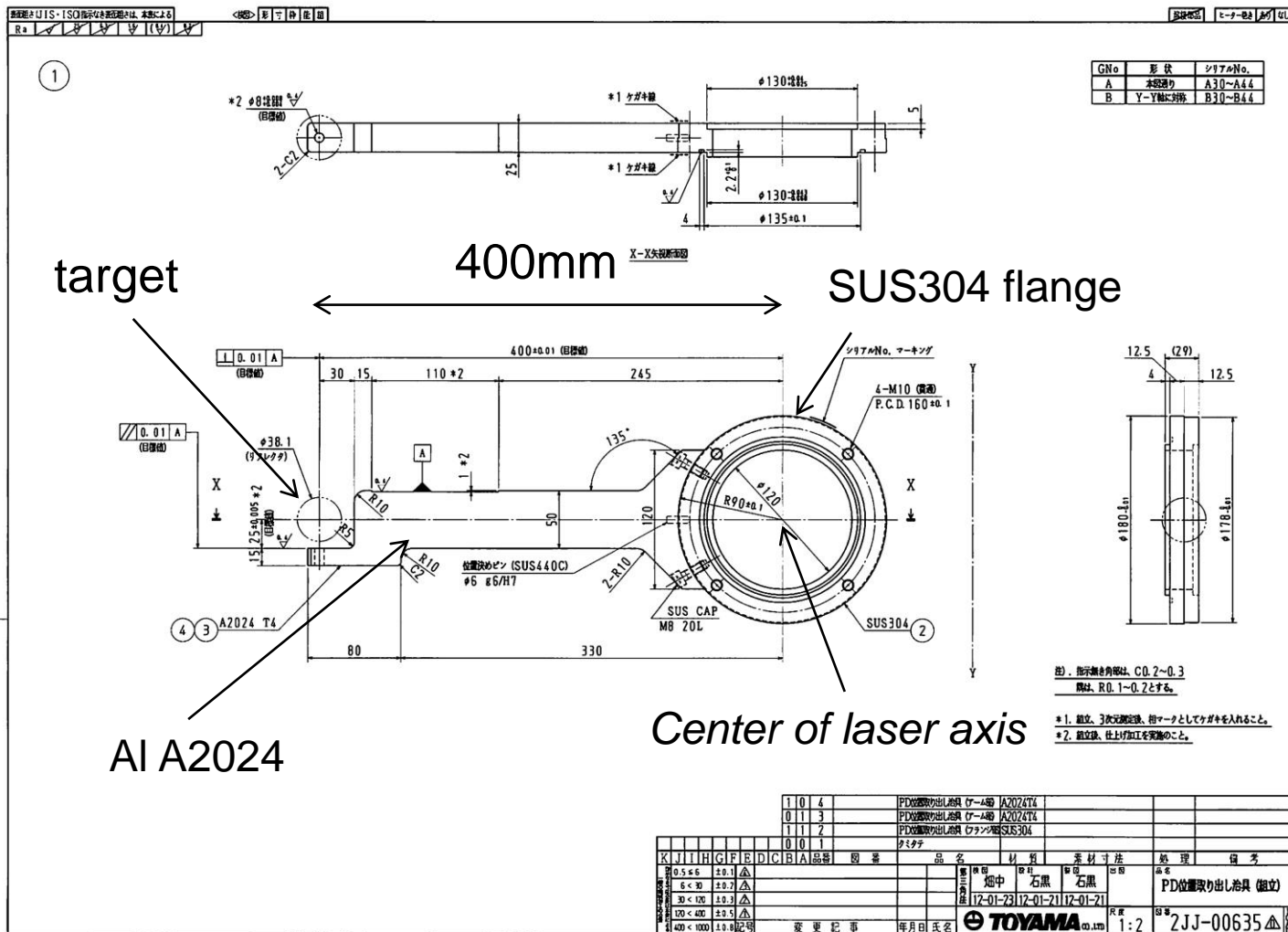
レーザーアライメント用基礎詳細図 8=1/30

※

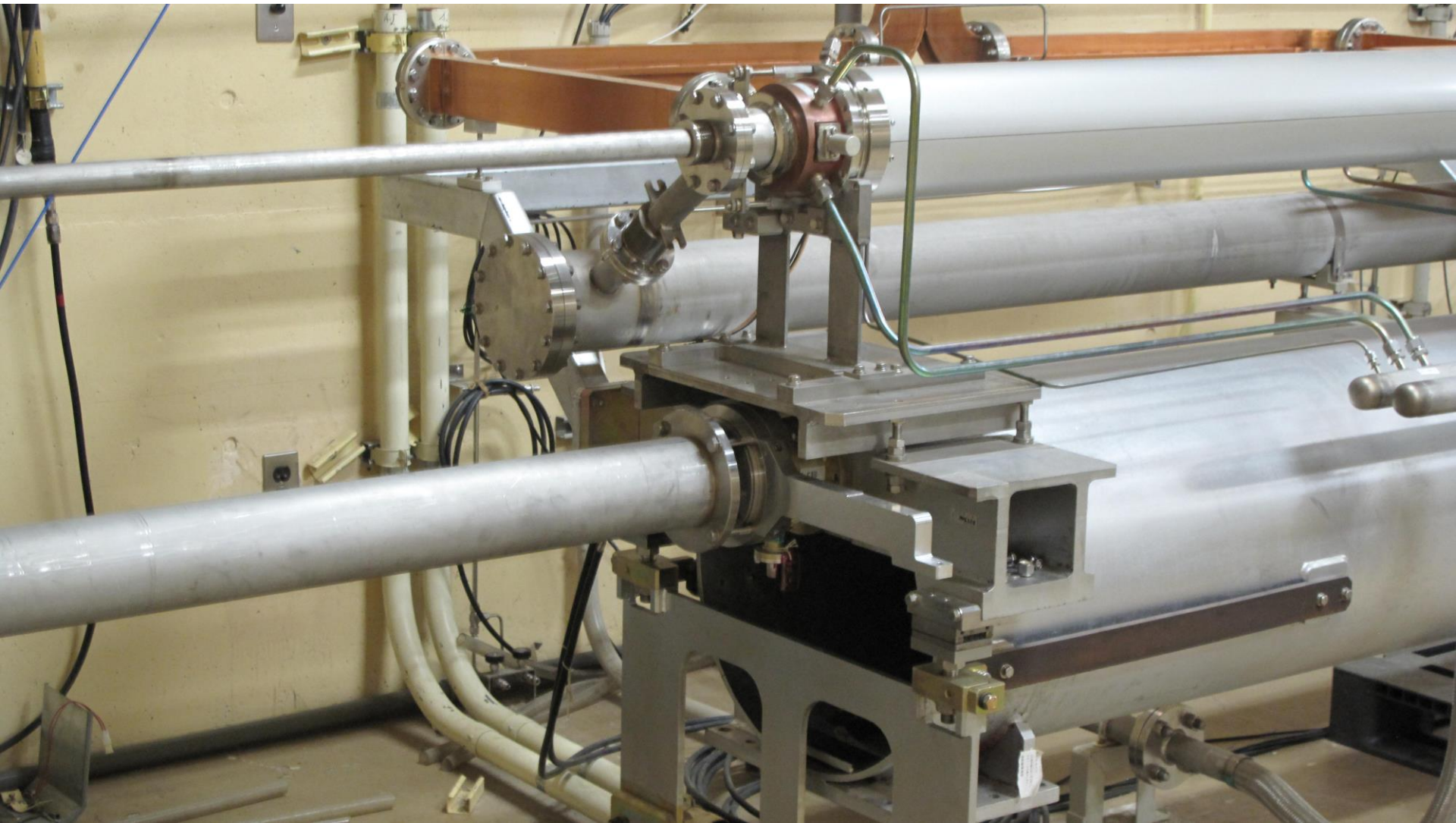
レーザーアライメント用基礎



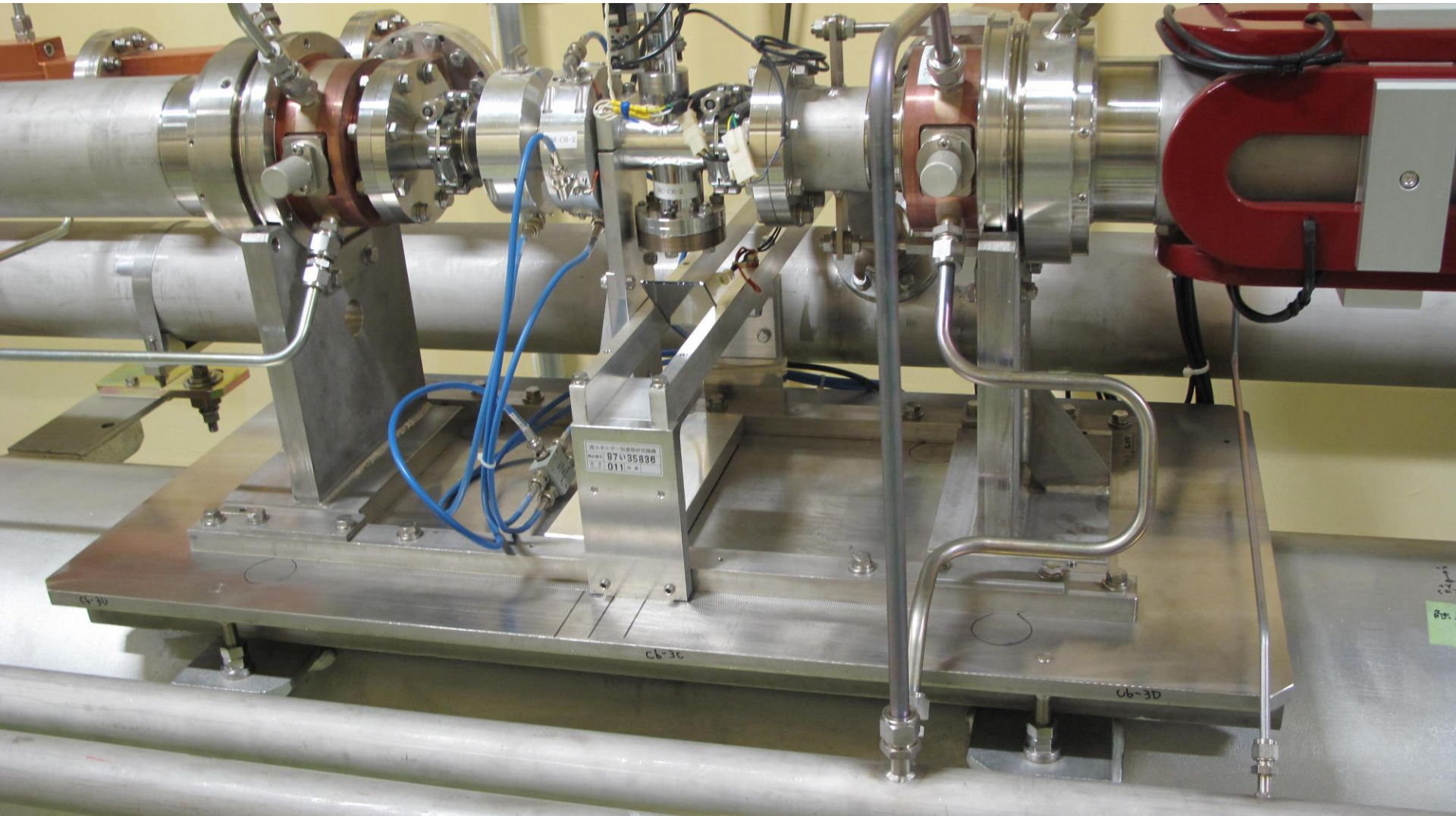
Mechanical jig for fiducialization of tracker target



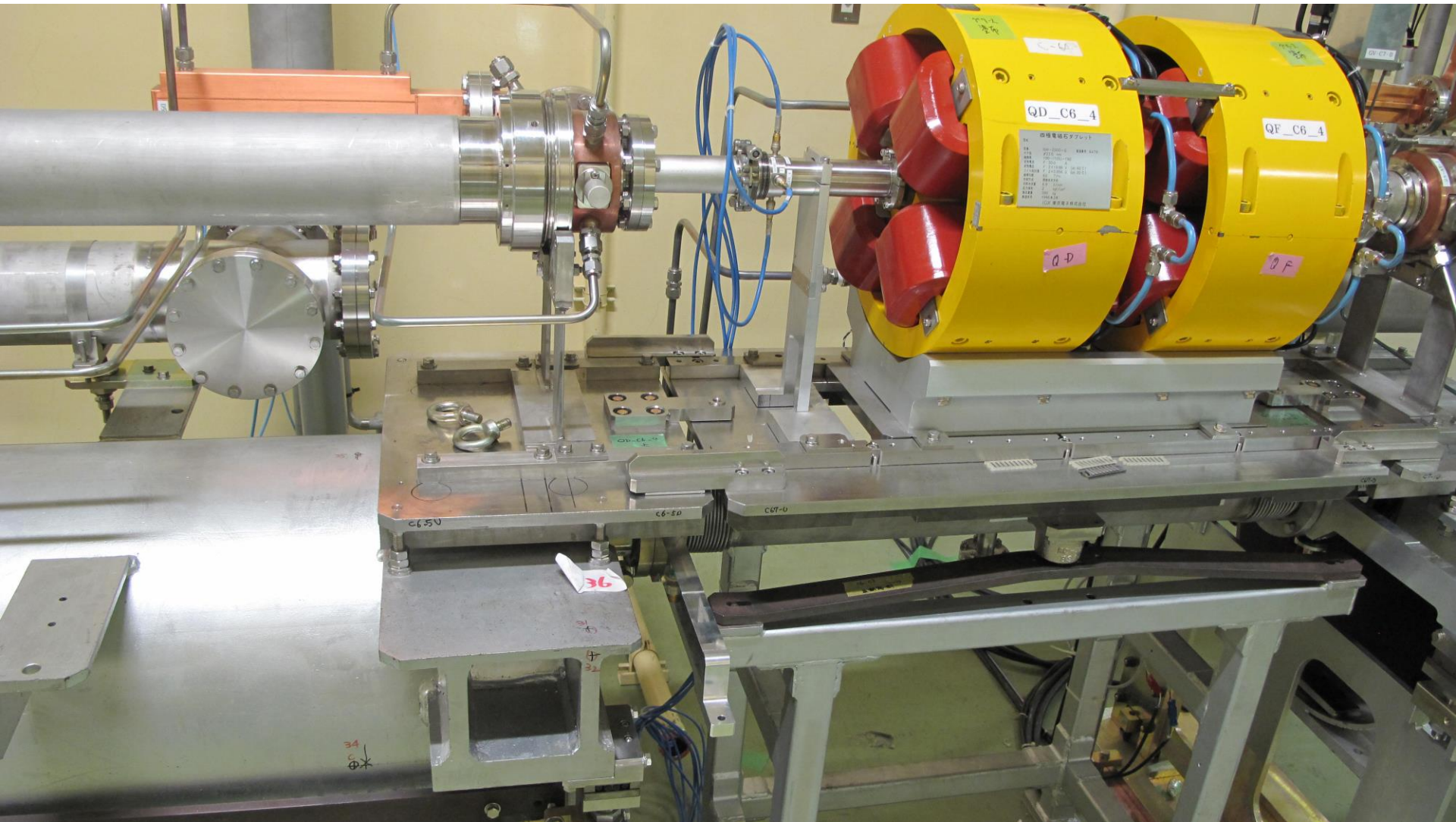
Laser pipe with a viewing port



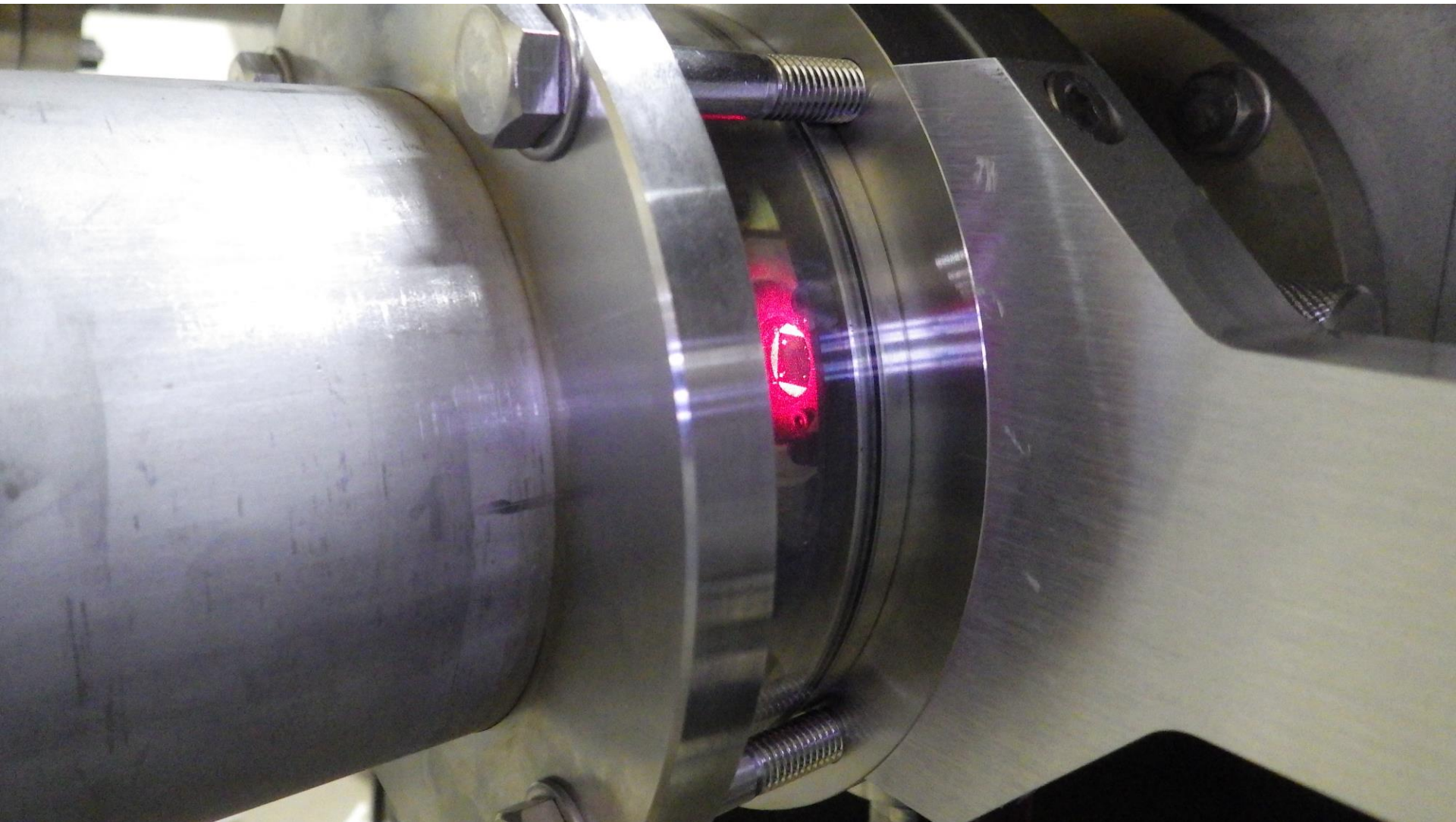
Support of accelerating structures



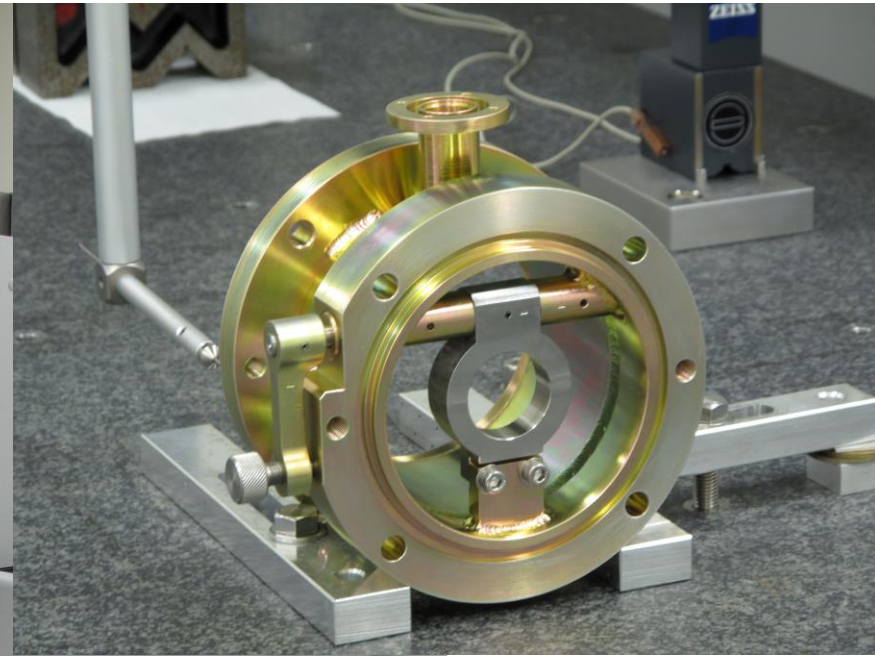
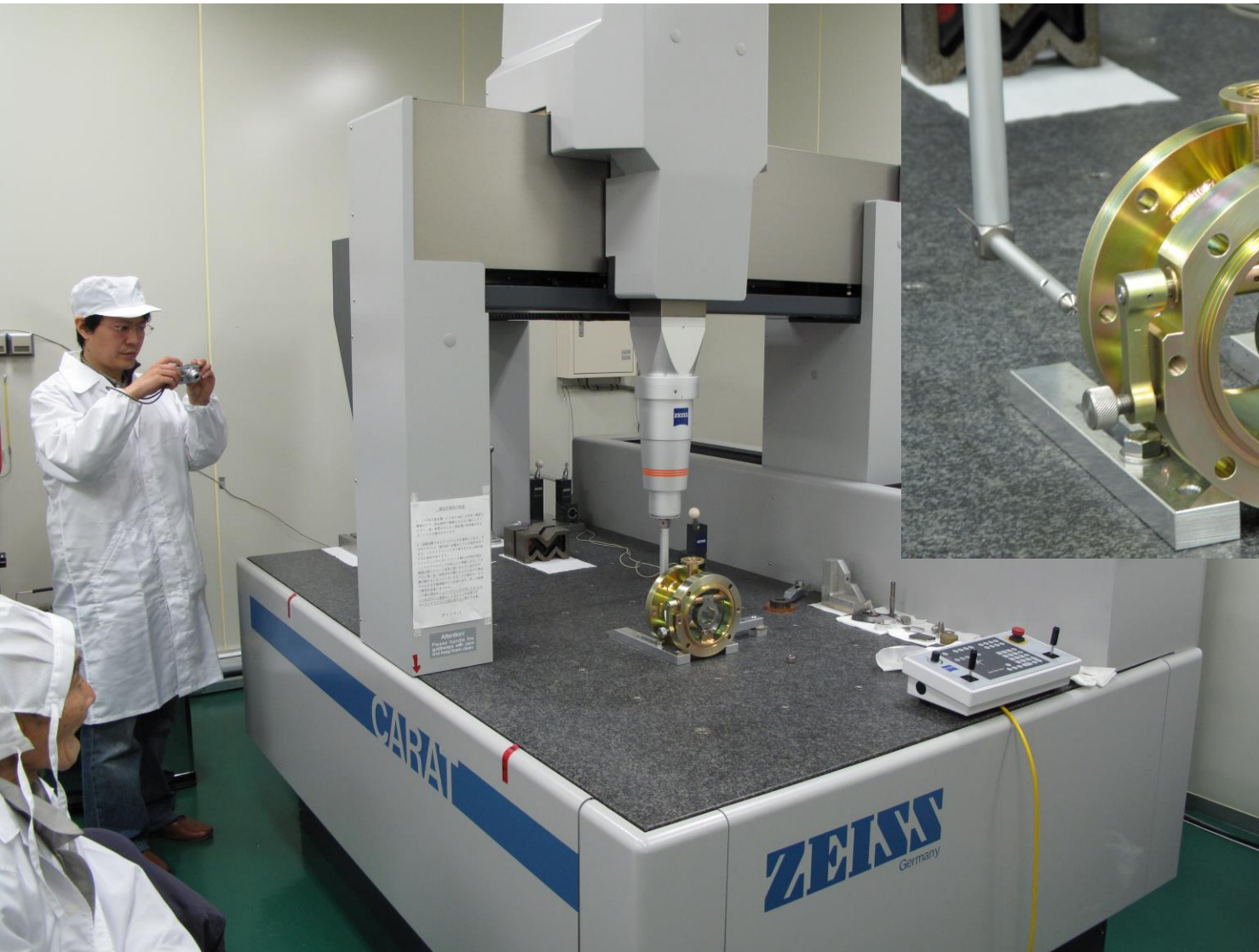
Connection between accelerating structure and Quad



Laser window



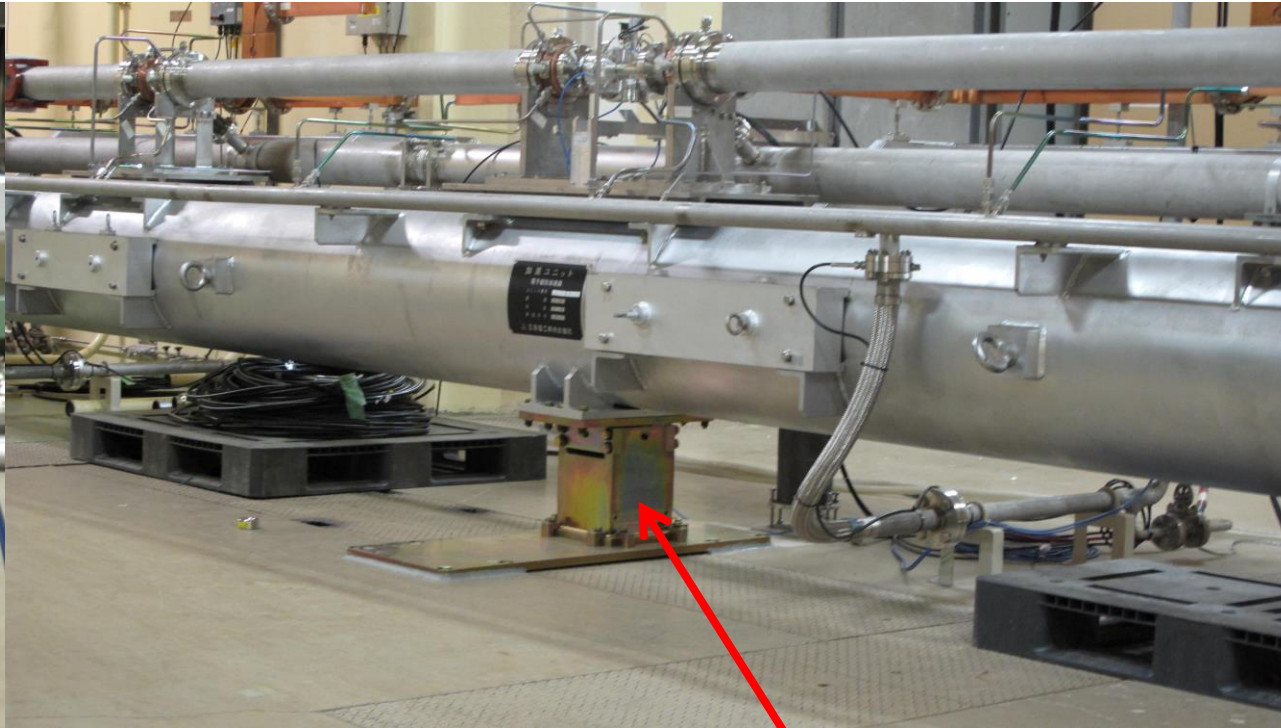
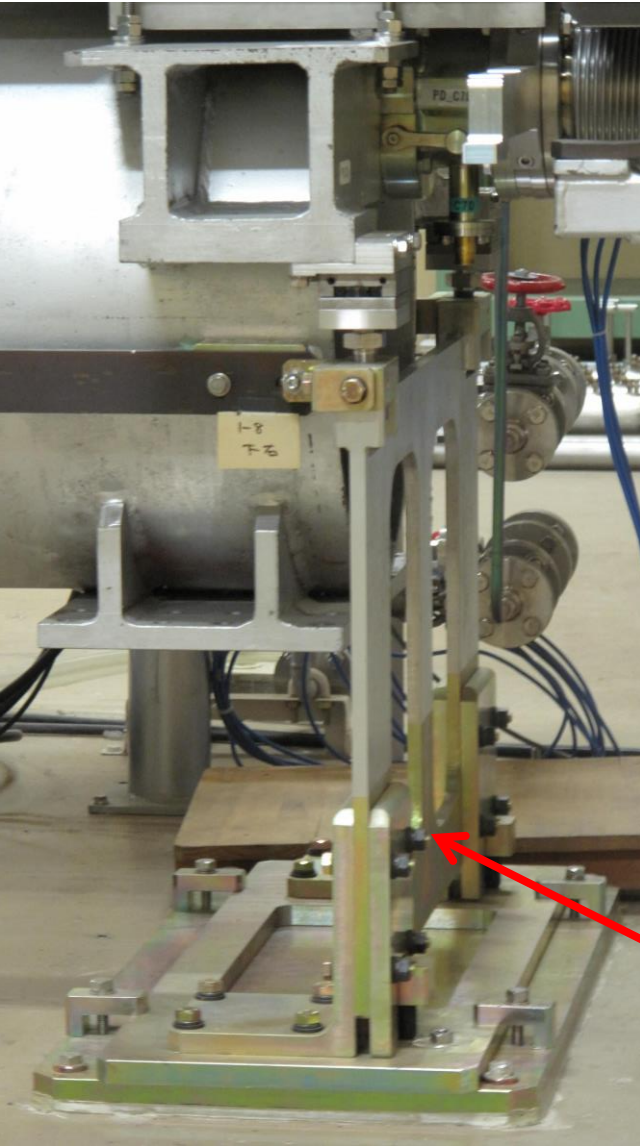
3D mechanical precision measurement in QPD holder



Test bench in QPD setting calibration



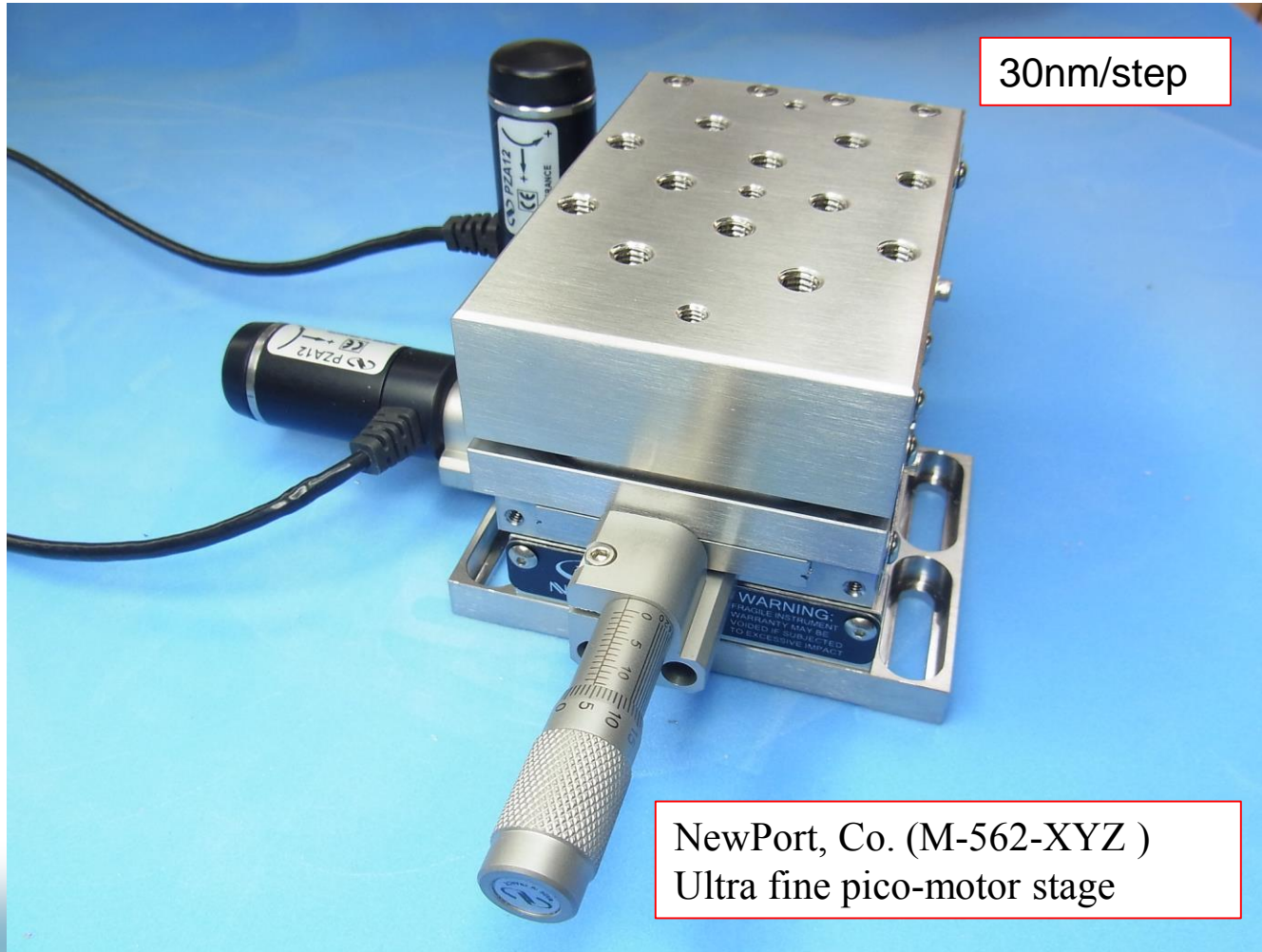
Reinforced girder



Center support added

Leg reinforced

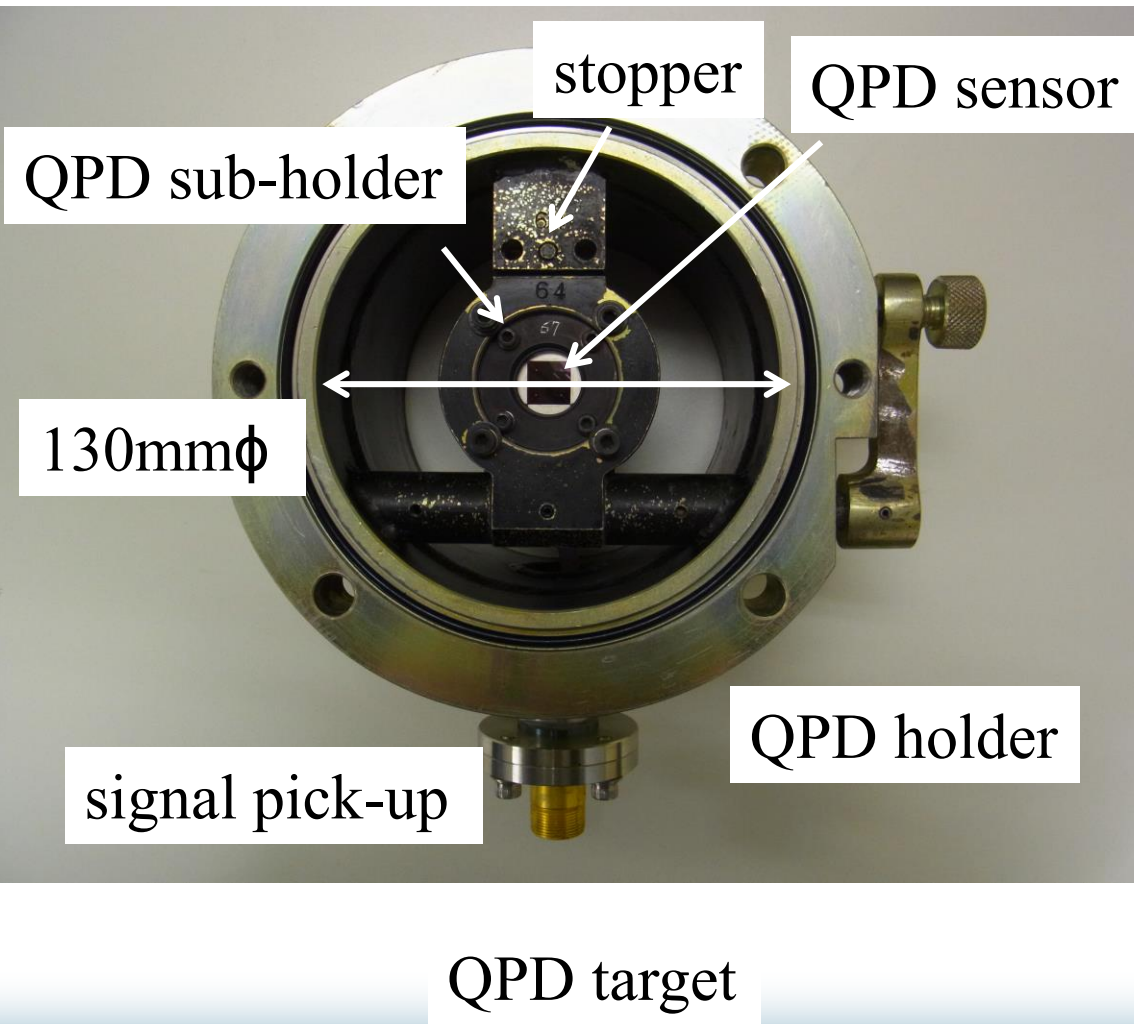
Ultrafine stage to stabilize the laser pointing



Laser system under operation



Quadrant Silicon Photo-Diode (QPD)



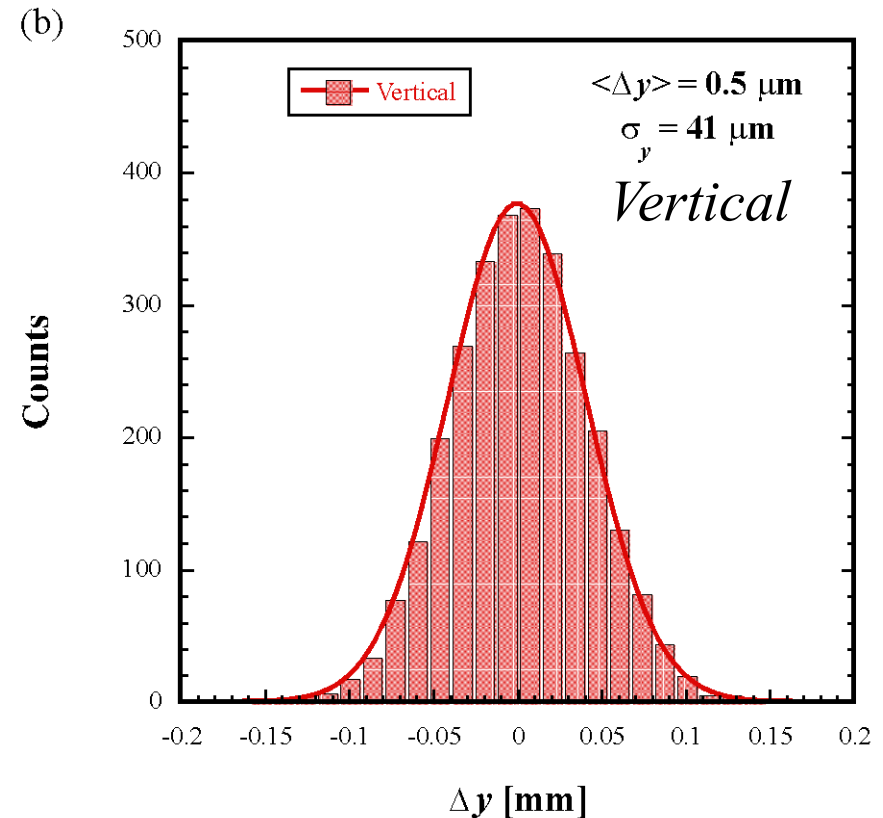
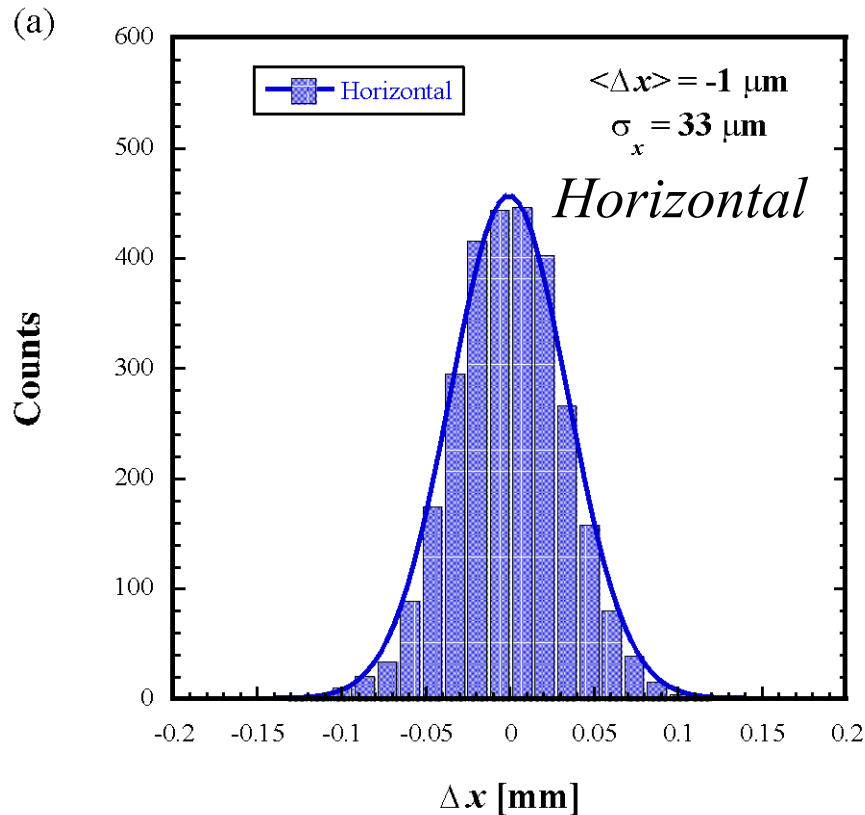
QPD: OSI Optoelectronics
SPOT-9D (D=10mm ϕ)

- QPD is mounted in the center of a sub-holder.
- The sub-holder can stand upright by rotation of a lever through hinge structure. The inner diameter of the holder is 130mm Φ .
- The QPD holder is connected to a laser pipe (SUS) by flange-flange joining.

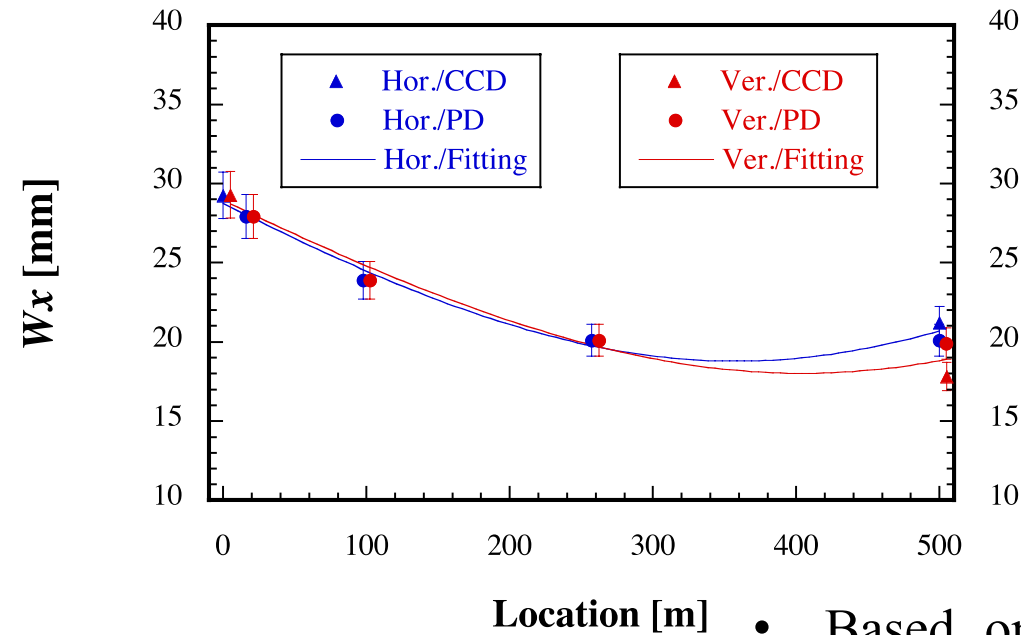
Developments for the laser-based alignment system

- s Our laser-based alignment system was first implemented at the construction stage in 1982; however, the high stabilization of the laser-based fiducial line has not been realized until now.
- s At long last, a laser line with high stabilization has been implemented as a 500-m-long fiducial line for alignments in March 2013.
- s We experimentally investigated the propagation and stability characteristics of the laser line passing through metallic pipes in vacuum.
- s Pointing stability at the last fiducial point with the transverse displacements of $\pm 40 \mu\text{m}$ level in one standard deviation by applying a feedback control was successfully obtained. This pointing stability corresponds to an angle of $\pm 0.08 \mu\text{rad}$. This system is now fully exhibiting the successful results for the high-precision alignment of the injector linac currently in progress.

Position stability of the laser axes at the last QPD ($z=500m$)



Results of the laser size measurements along the linac



- *Direct beam size meas.*
 Δ : with CCDs at two end points
- *Indirect beam size meas.*
 \bullet : by a mapping with a movable QPD in the x and y directions at the middle locations, while the laser axis is fixed

Fitting function

$$W_x(z) = W_{x0} \sqrt{1 + \left(\frac{z - z_{x0}}{z_{Rx}} \right)^2},$$

- Based on a least-square fitting procedure with standard Gaussian laser optics, the widths propagating along the z -axis were obtained as follow:

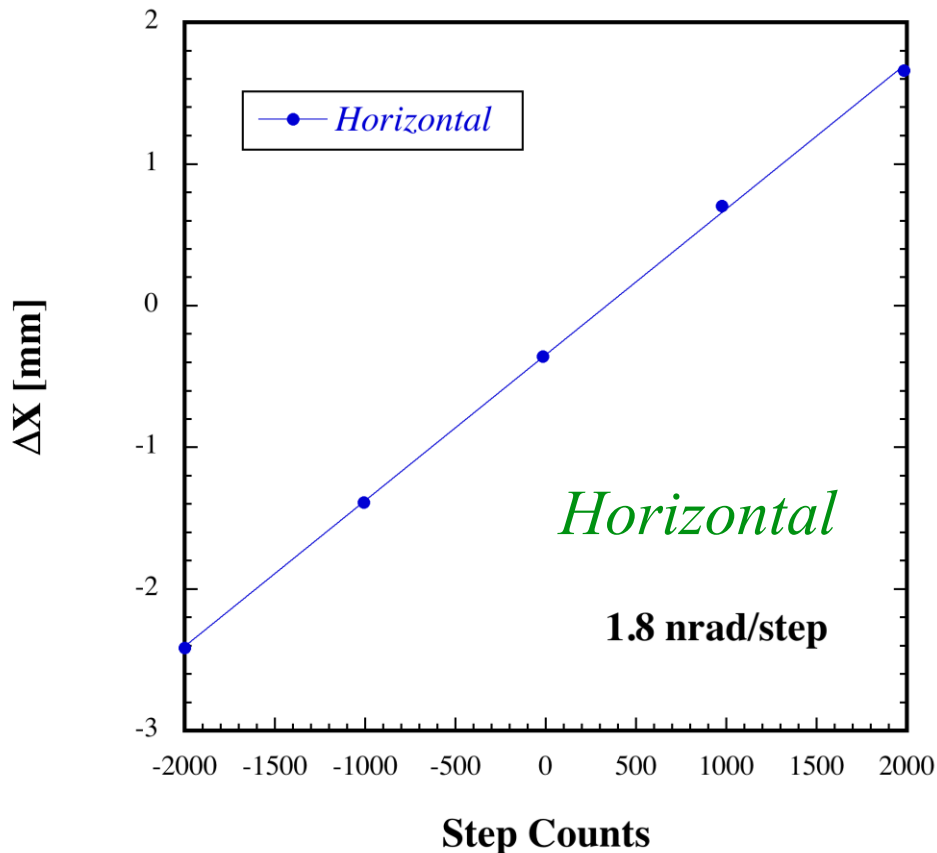
Rayleigh lengths $z_{Rx} \sim 308$ m, $z_{Ry} \sim 321$ m,

Waist locations $z_{x0} \sim 358$ m, $z_{y0} \sim 399$ m,

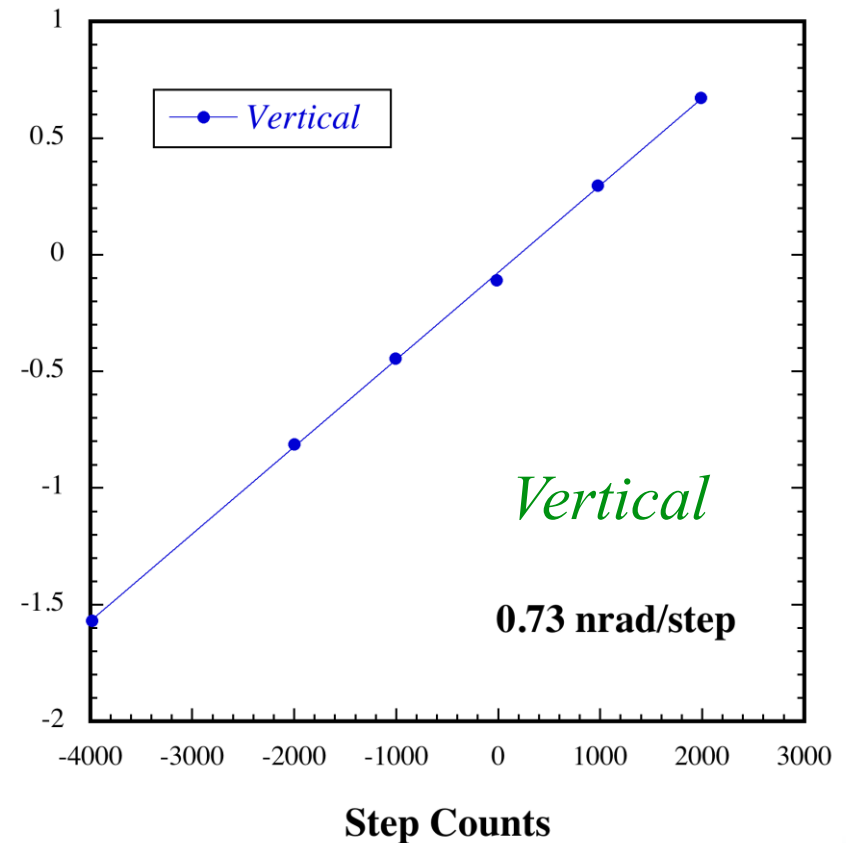
Beam sizes at waist locations $W_{x0} \sim 18.8$ mm, $W_{y0} \sim 18.0$ mm,

Sensitivity measurements of the laser axis at $z = 500m$

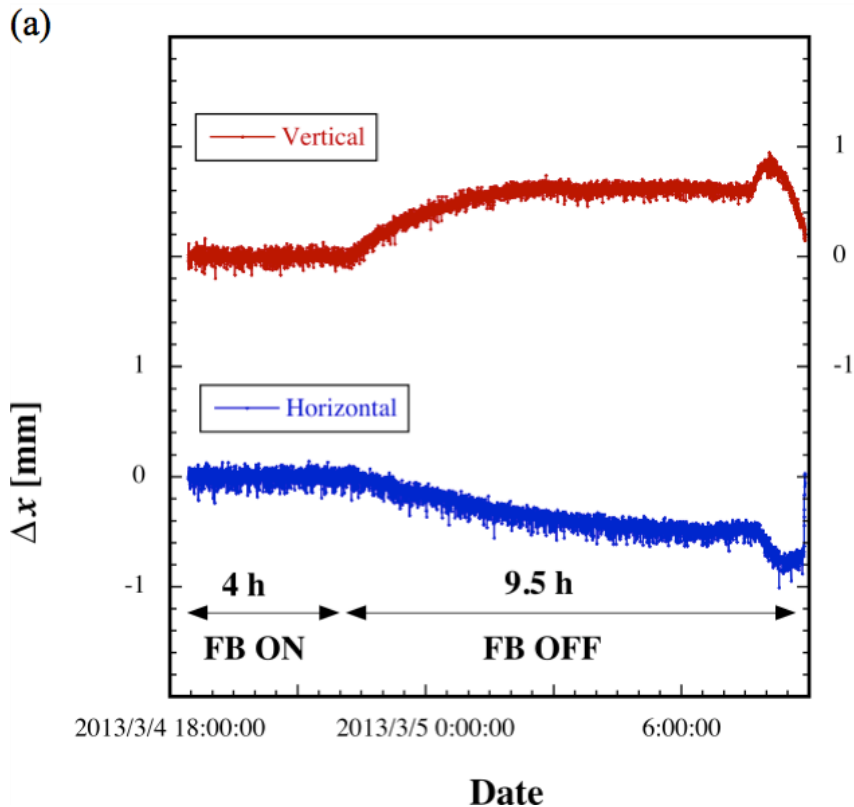
C5Laser X-Sensitivity Meas.



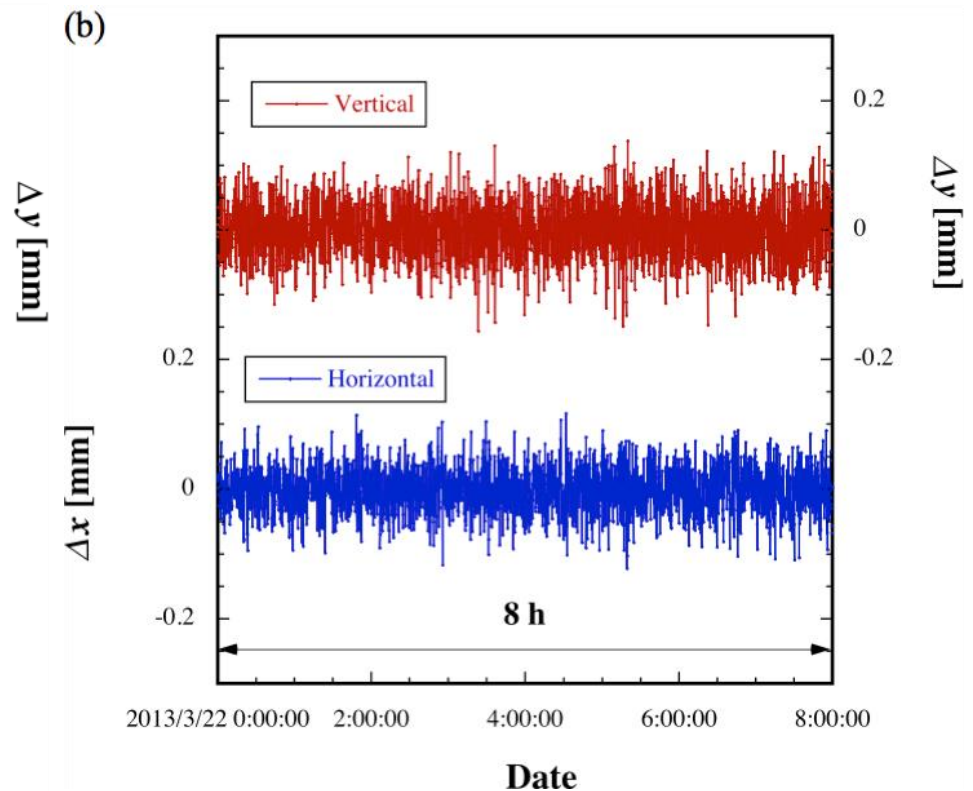
C5Laser Y-Sensitivity Meas.



Stability measurements of the laser axes at $z=500$ m



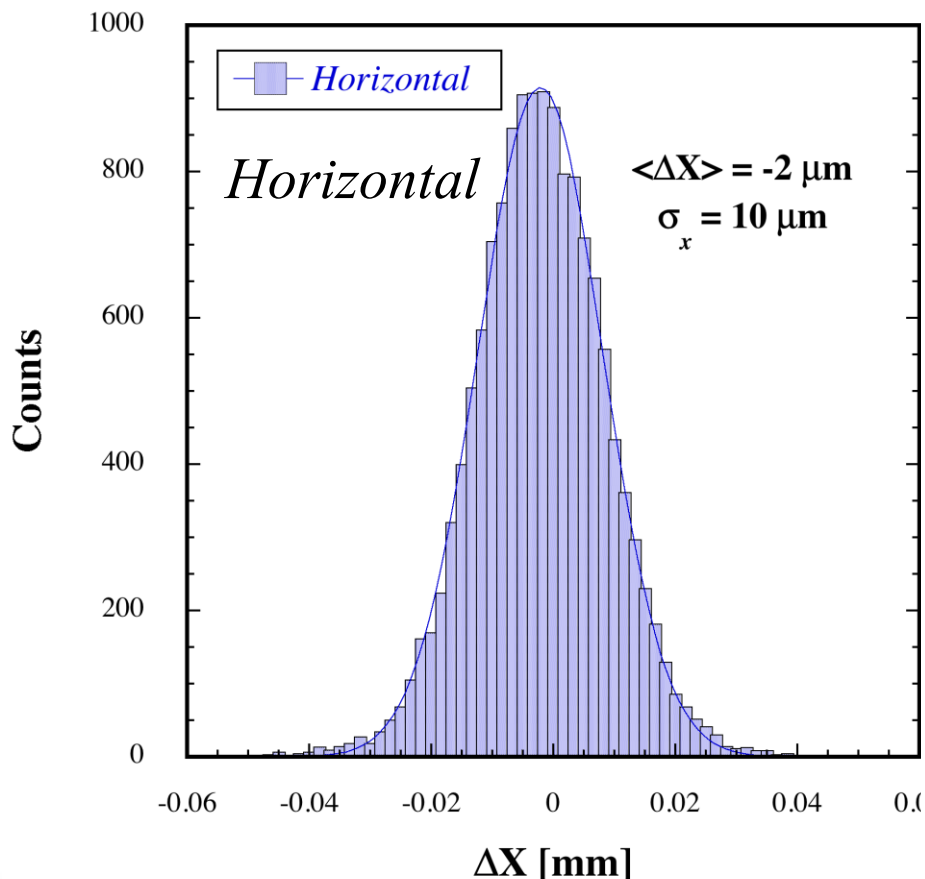
Time traces of the horizontal and vertical position displacements of the laser beam at the last QPD (a) with the feedback control on and off during 13.5 h



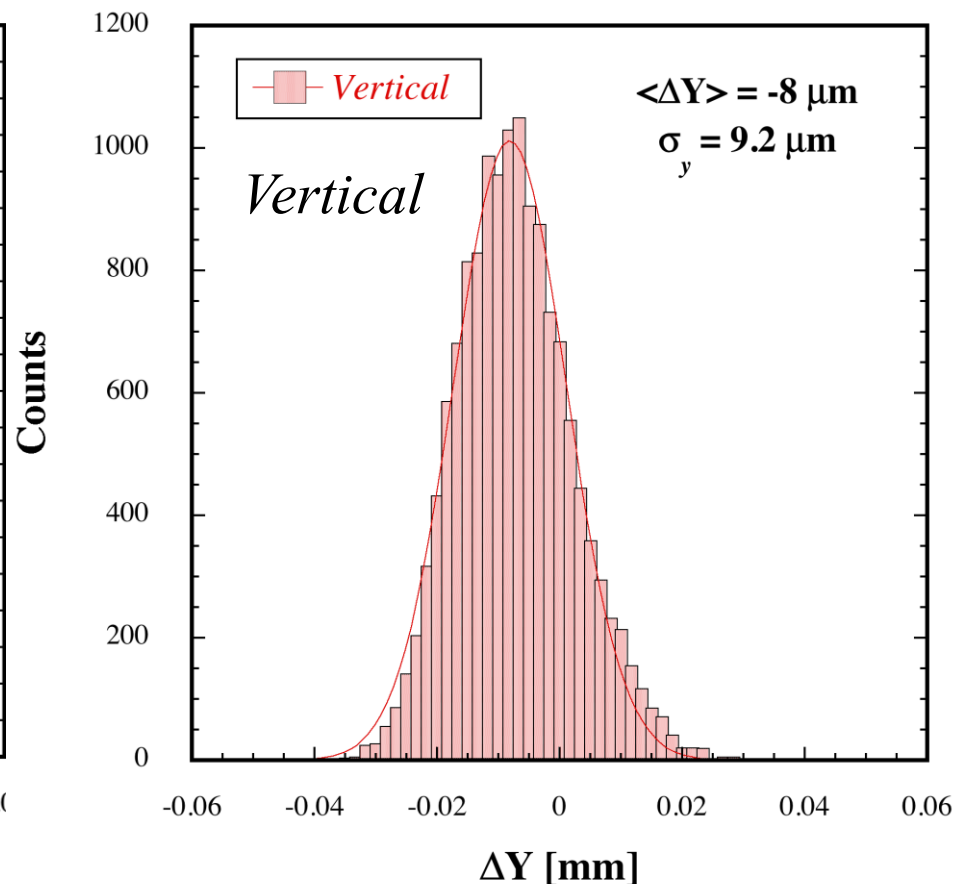
Time traces of the horizontal and vertical position displacements of the laser beam at the last QPD (b) with the feedback control on during 8 h.

Position displacement distribution of the laser axes for 132-m-long straight line

2013.July.12.AB.Laser



2013.July.12.AB.Laser



Expected error sources and estimations

Errors	Source of errors	rms error (μm)
--------	------------------	-----------------------------

Systematic error

Mechanical

- | | |
|-----------------------------------|----|
| • Mounting error of QPD | 10 |
| • Mounting error of QPD holder | 30 |
| • Reproducibility of QPD position | 30 |

Electrical

- | | |
|-----------------------------------|----|
| • Detection (offset) error of QPD | 12 |
|-----------------------------------|----|

Laser Shape

- | | |
|-----------------|----|
| • Profile error | 10 |
|-----------------|----|

Summation (rms sum)	46
---------------------	----

Statistical error

Laser stability

- | | |
|------------------------|----------|
| • Laser axis stability | ± 40 |
|------------------------|----------|